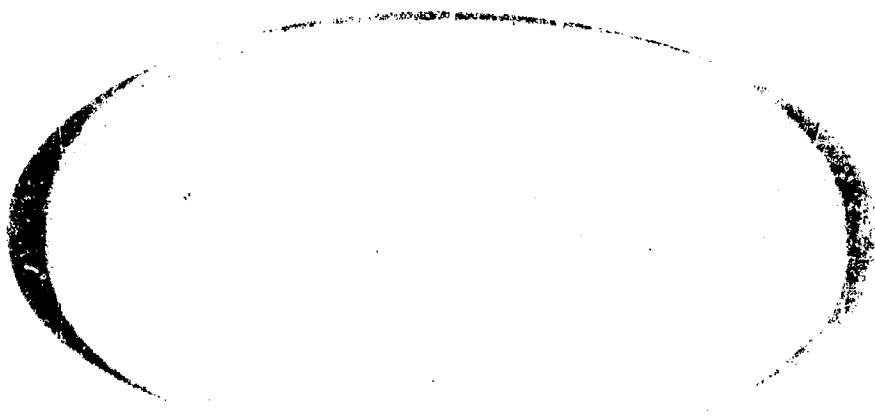


MILP Copy  
61-9 (cont.)



GPO PRICE \$ \_\_\_\_\_  
CSFTI PRICE(S) \$ \_\_\_\_\_  
Hard copy (HC) \$ 2.00  
Microfiche (MF) 1.50

ff 853 July 65

**N 65-33250**  
(ACCESSION NUMBER)  
49  
(PAGES)  
CR-64640  
(NASA CR OR TRX OR AD NUMBER)

\_\_\_\_\_  
(THRU)  
\_\_\_\_\_  
(CODE)  
14  
\_\_\_\_\_  
(CATEGORY)



**ENGINEERING  
PHYSICS**

**6515 RANDOLPH ROAD / ROCKVILLE, MARYLAND COMPANY**

ENGINEERING-PHYSICS COMPANY  
5515 Randolph Road  
Rockville, Maryland

INDUCTION FLOWMETER FOR DIELECTRIC FLUIDS

Experimental Verification

Final Report

by Vincent Cushing, Dean Reilly, and T. R. Schein

For

NATIONAL AERONAUTICS AND SPACE ADMINISTRATION

Contract NASr-53  
EPCO Project No. 105

April 16, 1962

ENGINEERING-PHYSICS COMPANY

## TABLE OF CONTENTS

	<u>Page No.</u>
LIST OF FIGURES .....	iii
I. INTRODUCTION .....	1
II. GENERAL DISCUSSION .....	4
A. Equivalent Circuit .....	4
B. Frequency of Operation .....	16
C. Input Equivalent Noise .....	17
D. Coarse Hum Compensation .....	18
E. Noise in Flowing Dielectric .....	19
F. Expected and Measured Voltages .....	21
III. FLOWMETER COMPONENTS .....	23
A. Housing and Fittings .....	23
B. Magnetic Circuit .....	26
C. Pipe/Transducer .....	30
D. Amplifier .....	37
E. Hum Compensator .....	40
F. Associated Electronic Equipment .....	41
IV. CONCLUSIONS AND RECOMMENDATIONS .....	43

LIST OF FIGURES

<u>Fig. Number</u>	<u>Page No.</u>
1. Equivalent circuit for electromagnetic flowmeter. Amplifier input equivalent circuit also shown.....	5
2. Graph of $\frac{\sin\beta}{E(\beta,1)}$ .....	7
3. Graph of $E(\beta,1)$ .....	8
4. Revised equivalent circuit for electromagnetic flowmeter .....	10
5. Approximate equivalent circuit for electromagnetic flowmeter .....	12
6. Approximate equivalent circuit for electromagnetic flowmeter, including driven-shield circuit .....	13
7. Approximate spectrum of electromagnetic noise .....	20
8. Meter housing .....	24
9. End fitting .....	25
10. Magnetic coil cross section .....	27
11. Coil winding technique .....	28
12. Intensity of magnetic induction transverse to pipe/transducer ....	31
13. Maximum magnetic induction measured along transducer axis as a function of the current in the magnetic coil .....	32
14. Electrode configuration of detection and driven-shield grids .....	34
15. End view of triaxial lead used to connect the pipe/transducer grids to the detection instrument .....	35
16. Meter pipe assembly .....	36
17. Schematic of amplifier used for detection of flow signal .....	38
18. Prototype flowmeter test circuit .....	42

FOREWORD

This is the final report of efforts conducted at the Engineering-Physics Company under Contract NASr-53. The objective of the work has been the experimental verification of prior theoretical and engineering efforts conducted for NASA by EPCO under Contract NASr-13.

The earlier engineering and theoretical effort indicated that an electro-magnetic flowmeter--with quite unusual performance characteristics--could be made to work with dielectric fluids such as petroleum products and the cryogenic liquids. Under the experimental verification effort, as reported herein, EPCO set up an instrumented fluid circuit (using petroleum base transformer oil as the fluid), and fabricated and tested the necessary components singly and in concert. These components were constructed essentially in conformance with the designs indicated in the final report to the effort conducted under Contract NASr-13.

The expected flow induced signal was successfully measured during the subject effort. Indeed, the overall performance of the dielectric induction flowmeter was essentially in conformity with the theory and analyses as developed in the above-mentioned prior effort. Based on the information gained during this experimental program, we are confident that an effort can now be fruitfully applied to the development of an operational flowmeter for the more difficult application of metering cryogenic liquids, including liquid hydrogen.

We should like to acknowledge the substantial advice and assistance of the project's technical manager, I. Warshawsky of the Lewis Research Center; and we are appreciative of the interest and close attention which has been given by the project manager, Henry Burlage, Jr. of NASA Headquarters' Liquid Rockets Section.

From the EPCO staff, the mechanical design work has been carried out by Leo Di Gioia; the attendant electronic devices have been constructed by William J. Tierney, Jr.; and the mechanical hardware has been fabricated by James R. Cullins.

Respectfully submitted,

ENGINEERING-PHYSICS COMPANY

*Vincent J. Cushing*  
Vincent J. Cushing

*Dean M. Reilly*  
Dean M. Reilly

*T. R. Schein*  
T. R. Schein

# INDUCTION FLOWMETER FOR DIELECTRIC FLUIDS--

## Experimental Verification

### Final Report

by Vincent Cushing, Dean Reilly, and T. R. Schein

#### I. INTRODUCTION

This is the final report on work conducted under Contract NASr-53--the work has consisted of an experimental verification of an induction flowmeter for use with dielectric fluids. On December 15, 1960, the Engineering-Physics Company initiated an engineering study for the subject flowmeter supported under Contract NASr-13. That engineering analysis indicated how an induction flowmeter could be made to work with dielectric fluids such as the cryogenic propellants. Conditions were prescribed whereby one might practicably detect the flow signal from such dielectric fluids, and designs for implementation were carried out. The engineering analysis effort was completed on March 15, 1961. On June 1, 1961, under the subject contract, the Engineering-Physics Company assembled, constructed, and tested the necessary components individually and in concert. The only serious difficulty encountered was in developing a practicable technique for fabricating the centrally important pipe/transducer configuration. When this difficulty was finally surmounted, the experimental verification phase moved along in straightforward fashion in accord with theoretical expectations; the expected flow induced signal--with flowing transformer oil, definitely a dielectric--was finally measured with repeatability in November 1961.\*

The utility of an electromagnetic flowmeter can be established from consideration of its two unique, advantageous characteristics:

1. obstructionless flow passage;
2. no moving parts.

As is now well-known, in the EM flowmeter the fluid encounters only a magnetic field; and it is the induced EMF which produces a measurement of the flow rate.

---

\* Predicated on the achievements as described in this final report, the Engineering-Physics Company at the time of writing has already embarked on the development of an electromagnetic flowmeter for use with liquid hydrogen--the program is conducted under NASw-381.

EMF measurement is made by means of detecting electrodes near the boundary of the fluid (in the design which we have formulated and successfully tested at EPCO, these electrodes do not even come in contact with the fluid, but are separated from the fluid by a thin teflon liner), and thus there is no probe or device of any kind which protrudes into the flow or disturbs the flow in any way. Thus there is no pressure drop in such a flowmeter. Furthermore, from the material standpoint, it is to be noted that the structural configuration--insofar as the flow is concerned--is simply a pipe: and with this simplicity there is today available a wide variety of chemically and physically refractive materials for especially difficult flowmeter applications. In these difficult applications (e.g., with liquid hydrogen or liquid fluorine) it is obviously advantageous to be without moving parts, bearings, etc. Finally, from the standpoint of dynamics, the lack of mechanical moving parts in the induction flowmeter provides unequalled sensitivity to flow oscillations; oscillations in fluid flow can therefore be detected and measured with limitations which are set only by the capabilities of the attendant electronic amplifier and detector.

The operability of the electromagnetic flowmeter for use with electrically conducting liquids has been well-known for many years, and indeed such flowmeters have been commercially available for use with such liquids for the past five or six years. However, there has long been an effort to make such a flowmeter operable with electrically nonconducting fluids such as petroleum base products (e.g., JP1, RP1, etc.); and very recently an effort to make the device operable with the decidedly dielectric cryogenic propellants. With electrically conducting fluids one makes use of induced conduction currents to provide the (signal) power necessary to actuate a suitable electronic voltage detector; and the novelty in the subject endeavor is that we have been able to make use of polarization currents in dielectric fluids in order to provide adequate power to actuate such an electronic voltage detector. Since it is a basic fact that polarization currents induced in a dielectric are proportional to the frequency of induction, it has been necessary to employ a high frequency magnetic field in this electromagnetic flowmeter for use with dielectric liquids. For a manifold of reasons--as discussed in Section II B of this report--we have for the purposes of this project compromised on an induction frequency of 10 kc per second.

During the conduct of the subject experimental effort, it has not been necessary to make any essential changes to the underlying theory or basic design aspects as reported earlier.<sup>1</sup> In accord with the terms of Contract NASr-53 it has been our objective in the work as reported herein to verify the operability of a volumetric flowmeter for use with dielectric liquids--and it is understandable that this should have been the first objective. However, it is perhaps worth noting here some of the important growth potential for the electromagnetic flowmeter.

As discussed in the final report to Contract NASr-13, it is fortunate for NASA's applications that hydrogen, oxygen, fluorine, nitrogen, and most of the constituents of RP1. consist of non-polar molecules. For these fluids one may introduce a simple compensation in the otherwise volumetric EM flowmeter based only on a measurement of bulk dielectric constant--and the flowmeter will thereafter read mass-flow directly.

Additionally, at a later date it would appear practicable to develop an electrical two-phase flowmeter system. As is well-known, the associated two-phase-high frequency magnetic induction is fully equivalent to a fixed magnetic field which rotates at the induction frequency. The net effect is that inhomogeneities in the flowing fluid are averaged out, and thus the electrical two-phase flowmeter would be capable of measuring flow rate in the face of hydrodynamically two-phase flow of arbitrary velocity profile.

Finally, as described in Section II A of this report, it appears possible to employ an electronic artifice in the EM flowmeter's attendant amplifier system such that the EM flowmeter can be calibrated once, and thereafter used indiscriminately with all variety of electrically conducting as well as dielectric fluids.

---

<sup>1</sup>Vincent Cushing and Dean Reily, "Induction Flowmeter for Dielectric Fluids--Engineering Analysis," Final Report issued by EPCO for Contract NASr-13, March 22, 1961.



## II. GENERAL DISCUSSION

Sections III and IV of this report describe in detail the individual components of the electromagnetic flowmeter and describe the test set-up and results obtained with the entire device. But here in Section II we should like to provide a discussion in general terms--indicating the theoretical expectations as compared with the observed performance.

### A. Equivalent Circuit

As described in the cited final report to Contract NASr-13 the equivalent circuit\* for the electromagnetic flowmeter is as indicated in Fig. 1; also shown there is the input impedance of the associated detecting amplifier. From the engineering analyses which have already been reported,<sup>2</sup> it has already been established that

$$e_f = \frac{BF}{a} \frac{\sin \beta}{E(\beta, 1)} \quad , \quad (1)$$

$$e_h = j\omega BM \quad , \quad (2)$$

$$R_f = \pi / [2\sigma LE(\beta, 1)] \quad , \quad (3)$$

$$C_f = 2(K - 1)K_o LE(\beta, 1) / \pi \quad , \quad (4)$$

$$C_s = 2K_o LE(\beta, 1) / \pi \quad , \quad (5)$$

where B is the magnetic induction in webers per square meter;  
F is the volumetric flow rate in cubic meters per second;  
a is the internal radius of the flowmeter pipe in meters;

---

\*For simplicity in discussion we describe here only a single-sided scheme. As described in Section III D of this final report, our actual flowmeter provides a push-pull output which is fed into a push-pull amplifier. The reader will have no difficulty in embellishing the discussion presented here to provide for a push-pull system.

<sup>2</sup>Final Report for Contract NASr-13, Section V, p. 32 ff, March 22, 1961.

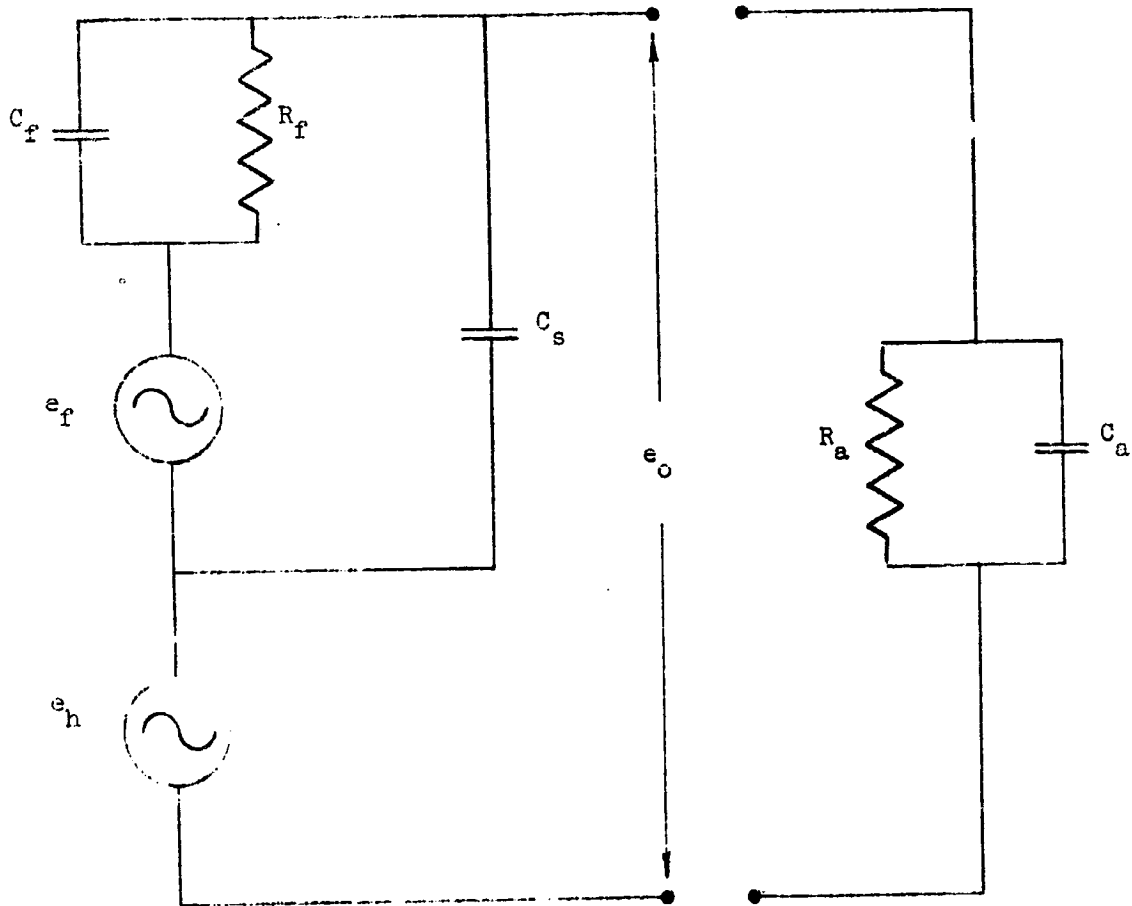


Fig. 1--Equivalent circuit for electromagnetic flowmeter.  
Amplifier input equivalent circuit also shown.

$\beta$  is the semi-angle subtended by each detecting electrode;

$E(\beta, k)$  is a tabulated<sup>3</sup> elliptic integral;

$j$  is the square root of  $-1$ ;

$\omega$  is the angular frequency of induction;

$M$  is a coefficient which depends only on the geometry of the overall flowmeter configuration;\*

$\sigma$  is the electrical conductivity of the metered fluid in mhos per meter;

$L$  is the length (along the axial direction of the flowmeter) of the sensing portion of the flowmeter in meters;

$K$  is the dielectric constant of the metered fluid, dimensionless;

$K_0$  is the permittivity of free space, 8.85 picofarads per meter.

The generator voltage,  $e_g$ , is the desired flowmeter voltage, being proportional to the volumetric flow rate,  $F$ . The generator voltage,  $e_h$ , is the undesired hum voltage generally to be expected due to "transformer effect" EMF generation--it is independent of the volumetric flow rate,  $F$ , and is proportional to the frequency of induction and also the amplitude of the magnetic induction. From Eqs. (1) and (2) we note that the hum voltage,  $e_h$ , is electrically in quadrature with the flow voltage,  $e_g$ .

In the subject project we are interested in metering dielectric fluids for which the electrical conductivity,  $\sigma$ , is negligible, so that  $R_p$ , the flowmeter's resistance, is virtually infinite. Under these conditions the internal impedance of the flowmeter, considered as an electrical generator, is entirely due to the flowmeter's capacitances,  $C_p$  and  $C_g$ . For the test fluid in this experimental effort we have employed a petroleum base hydraulic fluid, which has a dielectric constant of approximately 2.

---

<sup>3</sup>Jahnke-Emde-Losch, Tables of Higher Functions, Sixth Edition, McGraw-Hill Book Co., New York, 1960, p. 43 ff. (Also see Figures 2 and 3.)

\*In an ideal flowmeter the geometry would be perfectly balanced and symmetric such that the coefficient,  $M$ , would have the ideal value of zero--and in such an ideal configuration the undesirable hum voltage,  $e_h$ , would be non-existent. However, because of reasonable manufacturing tolerances, one must expect some geometric asymmetry with the result that the coefficient  $M$  is different from zero--and accordingly we must expect a certain amount of this undesirable hum voltage.

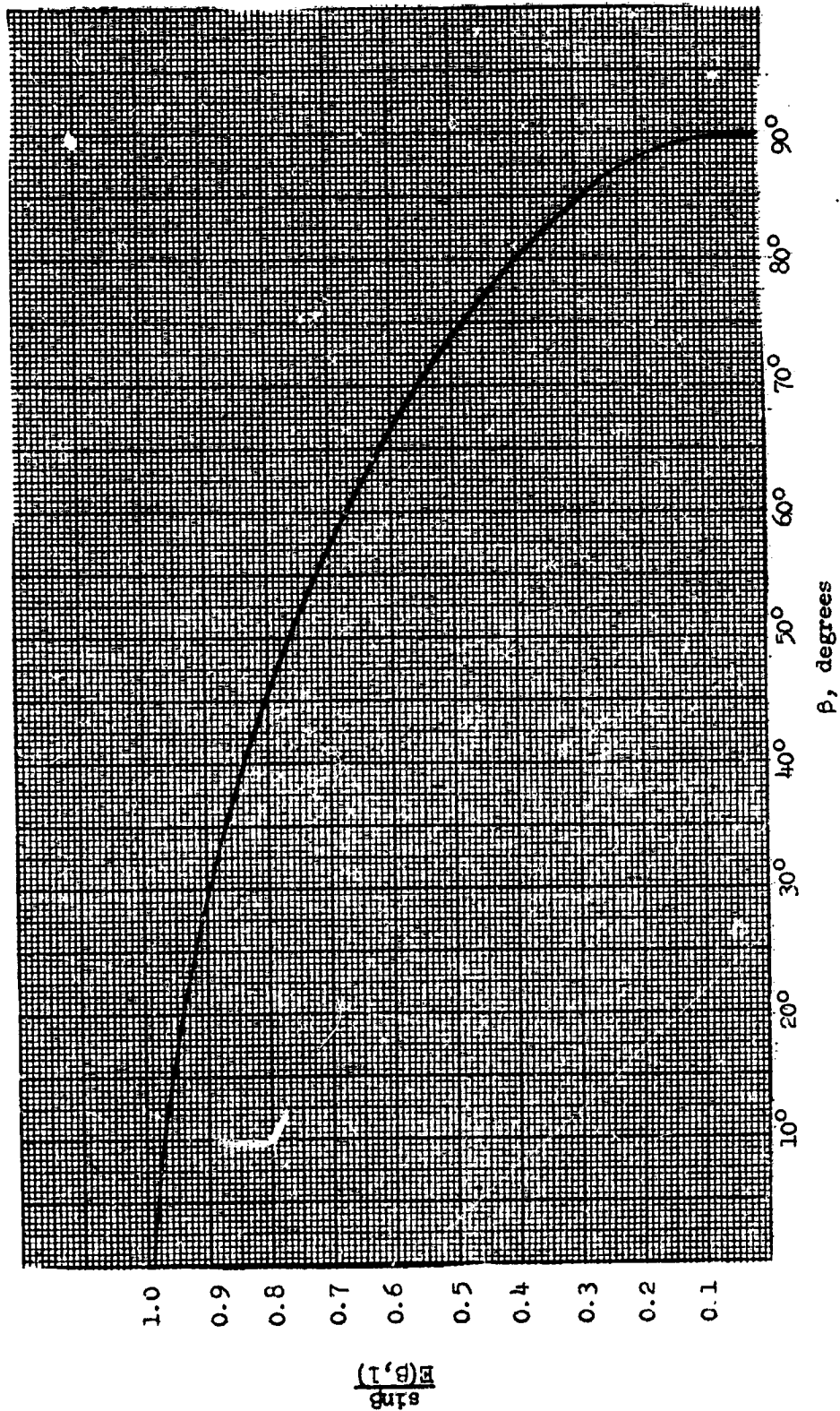


Fig. 2 --Graph of  $\frac{\sin \beta}{E(\beta, 1)}$  as a function of  $\beta$  where  $\beta$  is the semi-angle of the detecting electrode; and  $E(\beta, k)$  is a tabulated elliptic integral (see reference 3)

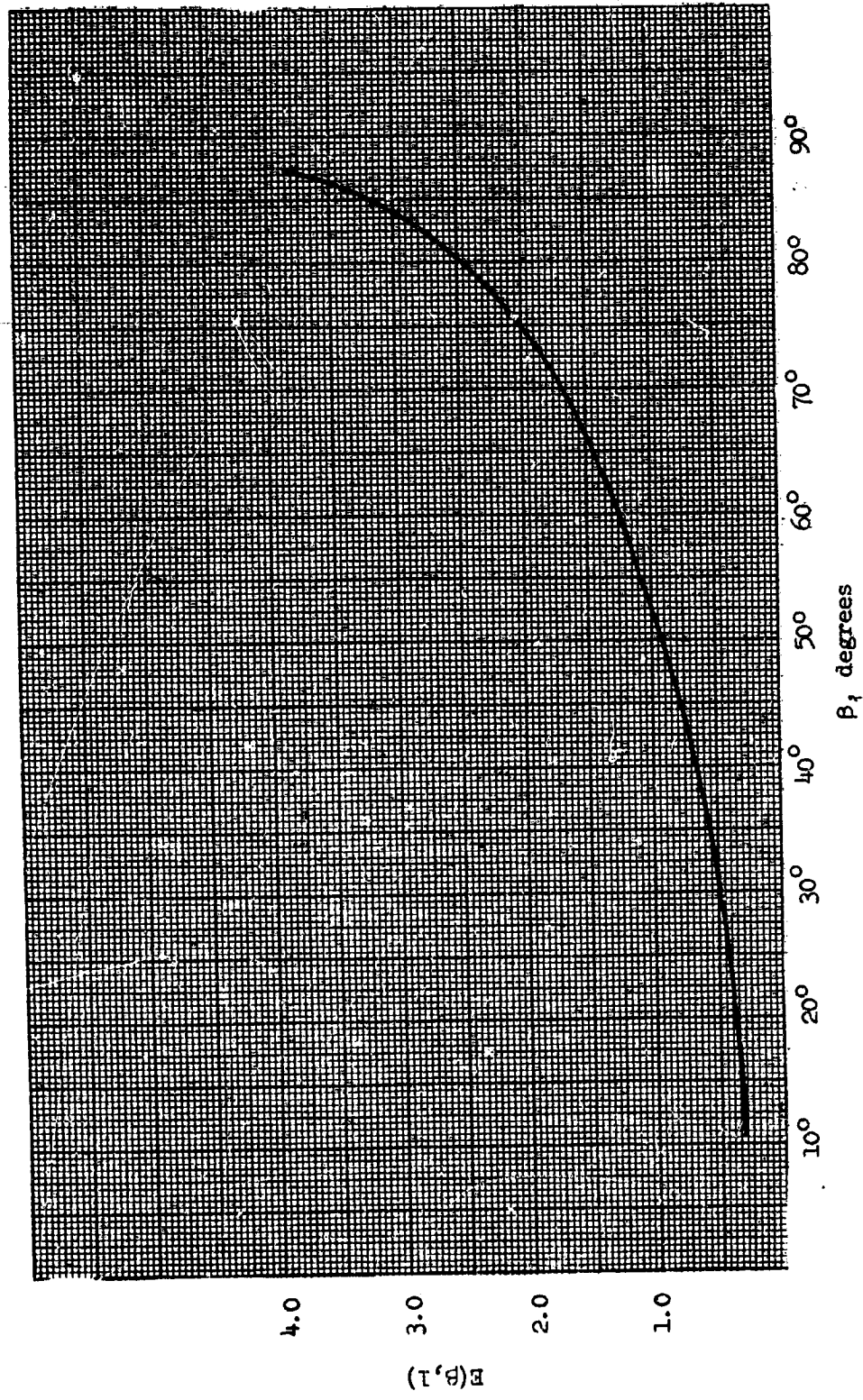


Fig. 3--Graph of  $E(\beta, 1)$  as a function of  $\beta$  where  $E(\beta, k)$  is a tabulated elliptic integral (see reference 3)

We have fabricated three detecting electrode configurations:\*

- Configuration 1                      length, L = 2 inches  
semi-angle,  $\beta = 50^\circ$  ;
- Configuration 2                      length, L = 3 inches  
semi-angle,  $\beta = 70^\circ$  ;
- Configuration 3                      length, L = 2.5 inches  
semi-angle,  $\beta = 85^\circ$  .

Using these data together with the information contained in Figs. 2 and 3, we find the following capacitances:

- Configuration 1                       $C_f = C_s = 0.28$  picofarads
- Configuration 2                       $C_f = C_s = 0.74$  picofarads
- Configuration 3                       $C_f = C_s = 1.15$  picofarads

Neglecting the flowmeter's resistance,  $R_f$ , we can evidently reconstruct the equivalent circuit of Fig. 1 into the simpler equivalent configuration indicated in Fig. 4. From this figure we see that the internal impedance of the flowmeter, considered as an electrical generator, is purely capacitive. For order of magnitude information we list below the internal impedance (a pure reactance), at frequencies of 10 kc per second and 100 kc per second, for the three electrode configurations cited above.

TABLE I  
Internal Reactance of EM Flowmeter

	<u>10 kc</u>	<u>100 kc</u>
Configuration 1	56 MΩ	5.6 MΩ
Configuration 2	22	2.2
Configuration 3	13	1.3

If we now wish to measure the flowmeter's output voltage,  $e_o$ , we must employ a high impedance voltmeter--i.e., a voltmeter whose impedance is large, say by a factor of 100, compared with the internal impedance of the flowmeter.

---

\* See Section III C of this report, and in particular, Fig. 15 . for terminology.

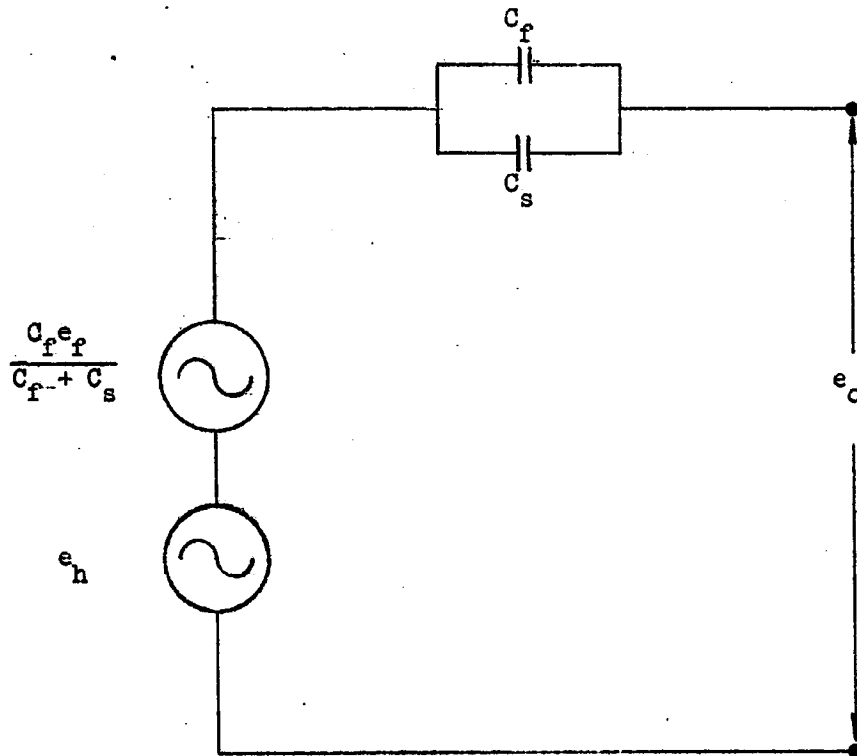


Fig. 4--Revised equivalent circuit for electromagnetic flowmeter.

Now, the input impedance of practicable vacuum tube voltmeters consists, as indicated in Fig. 1, of an input resistance,  $R_a$ , in parallel with an input capacitance,  $C_a$ . Typically, the input resistance,  $R_a$ , is indeed adequately large compared with the internal impedance values we have cited for our flowmeter;\* hence for the remainder of this discussion we will neglect the voltmeter's input resistance,  $R_a$ , and consider only its input capacitance,  $C_a$ .

If the voltmeter is now connected to the flowmeter, the overall circuit is as indicated in Fig. 5. From elementary circuit theory we determine that the measured voltage,  $e_a$ , is expressed by

$$e_a = \frac{C_f}{C_f + C_s + C_a} e_f + \frac{C_f + C_s}{C_f + C_s + C_a} e_h \quad (6)$$

From Eq. (6) we see that it is desirable to have the detecting voltmeter's input capacitance,  $C_a$ , as small as possible. As discussed in the final report to Contract NASr-13, the effective input capacitance,  $C_a$ , can indeed be made quite small by employing a driven shield configuration.

Such a driven shield configuration is described in detail in Section III D of this report; but here we should like to outline how such a driven shield can be used to advantage. Figure 6 is an embellishment of Fig. 5, but now showing additionally the capacitance,  $C_b$ , between the driven shield and the signal line. As indicated, the shield is driven by a voltage  $Ge_a$  from the output of the amplifier, whose gain is  $G$ ; for the moment we can make the reasonable approximation that the internal impedance of the generator,  $Ge_a$ , is negligible compared with the remainder of the impedances in the circuit. From straightforward circuit analysis we find the following expression for the amplifier input voltage or apparent voltage,  $e_a$

$$e_a = \frac{C_f e_f + (C_f + C_s) e_h}{C_f + C_s + C_a + C_b (1 - G)} \quad (7)$$

---

\* This is true, of course, only if the inductance frequency is adequately high. Since the internal impedance of our flowmeter is purely capacitive, its internal impedance varies inversely with induction frequency; hence, low frequency operation would not appear to be feasible.



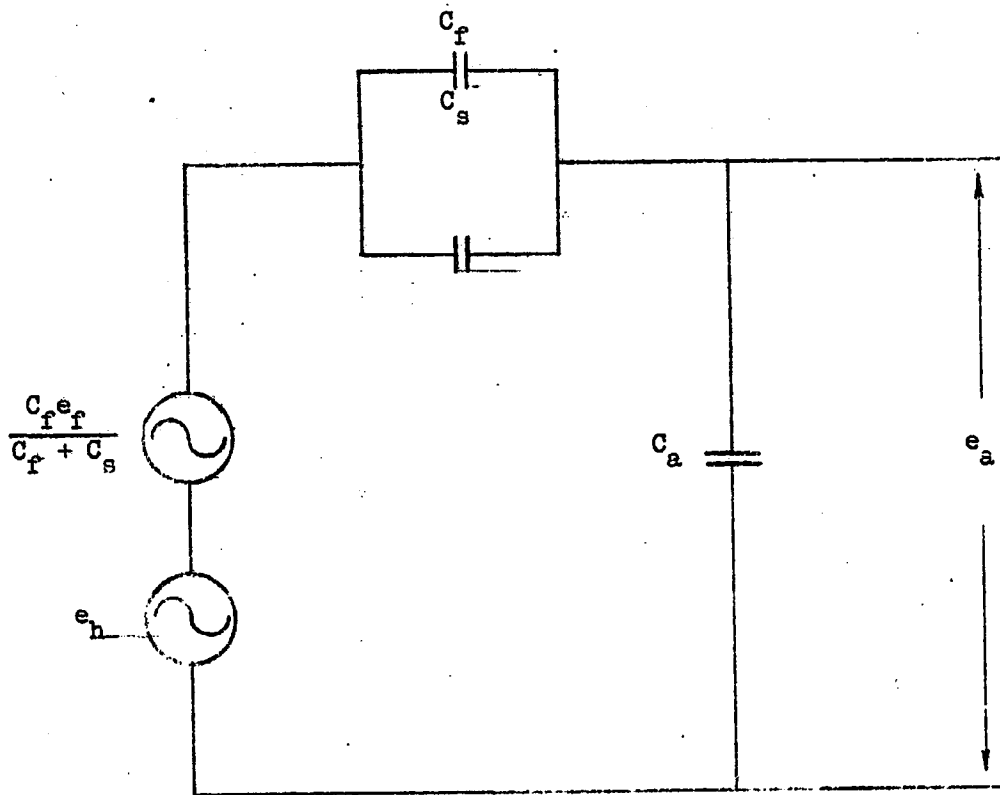


Fig. 5--Approximate equivalent circuit for electromagnetic flowmeter.

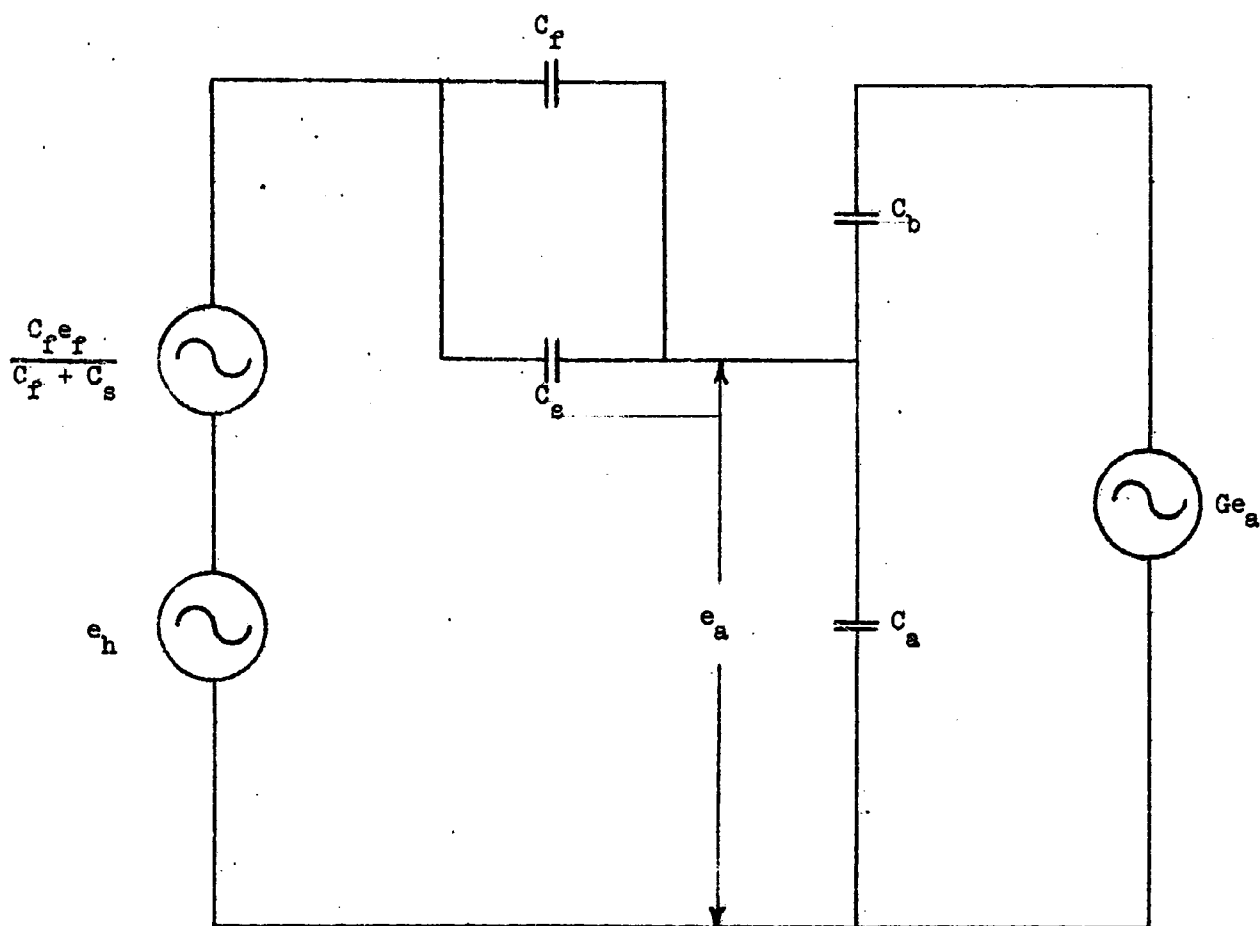


Fig. 6--Approximate equivalent circuit for electromagnetic flowmeter, including driven-shield circuit.

where the symbols are as indicated in Fig. 6. Now, if we set

$$C_s + C_a + C_b(1 - G) = 0 \quad , \quad (8a)$$

or

$$G = 1 + (C_s + C_a)/C_b \quad , \quad (8b)$$

then Eq. (7) becomes

$$e_a = e_f + (1 + C_s/C_b)e_h \quad . \quad (9)$$

Equations (8b) and (9) state that the measured voltage,  $e_a$ , will be equal to the flowmeter voltage,  $e_f$ , irrespective of the electrical properties of the fluid provided that the driven shield is driven from the output of a gain stabilized amplifier whose gain,  $G$ , is prescribed by Eq. (8b). In practice with our flowmeter the capacitance between the driven shield and the signal line,  $C_b$ , is something like 20-30 times as large as either of the flowmeter capacitances,  $C_s$  or  $C_a$ ; hence, the driven shield must be driven by an amplifier whose gain,  $G$ , is just slightly greater than unity. While this technique of somewhat overdriving the shield is very helpful in measurement of the flow induced voltage,  $e_f$ , it is not at all particularly helpful in suppressing the hum voltage,  $e_h$ --and indeed it appears from Eq. (9) that the hum voltage becomes somewhat augmented in the process, and so we must handle the hum problem by other techniques.

For a moment let us look at the above-described problem from the point of view of the apparent or effective input capacitance,  $C_a'$ , to the VTVM. Simple circuit analysis of the circuit indicated in Fig. 6 shows that the effective input capacitance,  $C_a'$ , is expressed by

$$C_a' = C_a + C_b(1 - G) \quad . \quad (10)$$

As discussed in Section III D of this report, the amplifier which we have constructed and employed in connection with the experimental verification effort for the electromagnetic flowmeter has an inherent input capacitance,  $C_a$ , of the order of 10 picofarads. But then, as described in Section III D, we adjusted the shield gain,  $G$ , from unity to values slightly above unity, and we were successful

in reducing the apparent input capacitance,  $C_a^i$ , down to the order of 1-2 picofarads, depending on the frequency of operation. Ideally, we note by reference to Eqs. (8a) and (10) that we should like to have  $C_a^i$  not only approach zero, but actually become somewhat negative. The fact that we were not able to achieve this with the first amplifier we believe is due to the fact that we have not yet considered the effects of phase shift in the amplifier. But nonetheless, our experience with this amplifier does demonstrate that, by the technique of slightly overdriving the driven shield, we are able to obtain at least a five- or ten-fold reduction in VTVM input capacitance.

We should now make a brief analysis of the effect of phase shift in the amplifier. To do this we simply express the driven shield amplifier gain,  $G$ , as the complex number

$$G = Ae^{j\theta} = A(\cos \theta + j \sin \theta) \quad , \quad (11)$$

where  $A$  is the amplitude gain of the amplifier;

$\theta$  is the phase shift associated with the driven shield amplifier.

We now insert Eq. (11) into Eq. (10), and write the real and imaginary portions separately--they are

$$\text{Re}C_a^i = C_a + C_b(1 - A \cos \theta) \quad ; \quad (12a)$$

$$\text{Im}C_a^i = -C_b A \sin \theta \quad . \quad (12b)$$

Within the framework of this perhaps overly simplified analysis here, we see from Eq. (12a) that the purely capacitive component,  $\text{Re}C_a^i$ , can still be adjusted to zero or even negative values by adjusting for the proper amplitude value of the amplifier gain,  $A$ . But from Eq. (12b) we note that an imaginary component of capacitance is generated; and in any circuit--an imaginary capacitance would have the effect of showing up as an imaginary reactance, i.e., a resistance. It is not surprising, then, that a bridge measurement of the effective input capacitance,  $C_a^i$ , would not indicate more than the above-cited ten-fold reduction in effective input capacitance--and even more it is not surprising when one considers that the measured values, 1-2 picofarads, are near the limit of resolution of the bridge employed. The analysis indicated here is merely meant to show the major

outline of the problem; clearly, an exact solution, taking into account all existing impedances including the resistive components,  $R_f$  and  $R_a$ , as indicated in Fig. 1, would yield a much more complex solution.

But even though a thorough analysis, including consideration of all impedances in the amplifier, the flowmeter, and attendant circuitry may be quite complicated, nonetheless the solution of the phase-shift problem is physically simple. In any flowmeter for practical operational use, we will operate at a fixed frequency, and hence suitable attention can be given to adjusting the phase shift of the amplifier adequately close to zero at that fixed frequency. In the experimental verification work reported here, however, one of the facets being investigated was the effect of induction frequency, and accordingly we employed a relatively wideband amplifier, having a frequency response from some 5 cps to  $10^6$  cps. Providing for a means of adjusting amplifier phase shift throughout this frequency spectrum was simply impractical in the present investigation; and we were satisfied to be able to reduce the effective input capacitance of our VTVM to the values required for experimental detection of the flowmeter signal induced in the flowing dielectric.

#### B. Frequency of Operation

During the engineering analysis as indicated in the final report to Contract NASr-13, it appeared that, since the internal impedance of the flowmeter--considered as an electrical generator--was purely capacitive, then the magnitude of the internal impedance would be low if the frequency of operation were quite high. For this reason we had originally considered operation of the electromagnetic flowmeter at frequencies as high as one megacycle per second. Thereafter, however, further consideration of the overall circuitry, including the input impedance of the attendant voltmeter as described above and indicated in Fig. 1, showed that insofar as impedance levels were concerned the problem was quite symmetric between the flowmeter and its attendant amplifier, so that frequency of operation insofar as this matter is concerned is irrelevant--that is to say, high frequency operation, to be sure, reduces the internal impedance of the flowmeter considered as a generator, but at the same time this same high frequency operation decreases the input impedance of the attendant amplifier.

There is, though, a lower limit of operating frequency: to obviate phase shift problems we would in any event like to operate at a frequency sufficiently high such that the amplifier's input (capacitive) reactance is small compared with the input resistance. With the induction flowmeter we have been testing during the subject experimental project, this consideration sets a lower limit of operation at about 1-5 kc per second.

A second requirement which may set the frequency of operation is the desired flow oscillation response time. It is readily seen that a flow oscillation amounts to an amplitude modulation of the average or steady flow induced voltage. The steady flow induced voltage is, of course, at the same frequency as the frequency of the magnetic induction; hence, the flow oscillation amounts to the generation of sidebands about this central induction frequency. Now, for high fidelity amplification of any amplitude modulated signal it is generally wise, as a rule of thumb, to have the carrier frequency at least 50-100 times higher than the modulation frequency. If such is the case, we essentially have a relatively narrow-band amplifier, with consequent advantages. In the case of the flowmeter this means that a 10 kc per second induction frequency will practically permit the resolution of 100-200 cps flow oscillations--and this is adequate for a first objective. However, if at a later date the flow oscillation sensitivity requirement climbs to, say, 1000-2000 cps, then it would appear wise to raise the induction frequency to the neighborhood of 100 kc per second.

#### C. Input Equivalent Noise

Because one of the objectives in the experimental project has been the evaluation of electromagnetic flowmeter performance for various operating induction frequencies, we have employed for experimental facility a relatively wideband amplifier, having a bandwidth extending from approximately 5 cps to  $10^6$  cps. It is well known that amplifier input noise is proportional to bandwidth; and with the wideband amplifier which we have employed in this experimental program this input equivalent noise was in the neighborhood of 30 microvolts. In any operational flowmeter, we will employ a fixed-frequency system, with a bandwidth only wide enough to provide proper response for the desired flow oscillation sensitivity. Thus, in any operational model the bandwidth of the amplifier need

only be somewhere in the neighborhood of 500-2000 cps--and accordingly the input equivalent noise level can be expected to be in the neighborhood of one microvolt or less.

D. Coarse Hum Compensation

As indicated in Eq. (7) [or Eq. (9)] there is in addition to the desired flow signal,  $e_f$ , an undesired hum voltage,  $e_h$ . Happily, as indicated by Eq. (2) this hum voltage is electrically in quadrature with the flow voltage,  $e_f$ . In principle, then, it is possible to employ a phase-sensitive detector which will accept the in-phase flow voltage,  $e_f$ , but at the same time reject or discriminate against the quadrature hum voltage,  $e_h$ . In practice, the hum voltage,  $e_h$ , can be of very sizeable magnitude--in the subject project we have experienced uncorrected hum voltages which are something like 10-20 times as large as the maximum flow voltage. In any further development program an effort should be made to control fabrication asymmetries; because careful balance in the circuitry can do much to reduce this hum voltage down to the same order of magnitude as the maximum flow voltage or perhaps much less. However, in the present experimental program the overall flowmeter configuration did not permit physical adjustment of the components to seek such a hum minimization; and consequently we had to rely entirely on the injection of an electrical compensating signal into the grid of the first stage of our detecting amplifier. The reason for wanting the hum voltage to be almost the same order of magnitude as the maximum flow voltage, is that the amplifier will behave in a linear fashion only provided it is not saturated by some extraneous voltage--for if the amplifier became saturated the final use of a phase-sensitive detector would be entirely useless.

The design of the hum compensation circuitry is described in detail in Section III E of this report. This hum compensation network permitted a manual adjustment of both the magnitude and phase of a compensating signal. By this means we were able to reduce the net hum to levels which fell well below the noise level of the amplifier we were using; it is estimated that even this manual compensation technique permitted reduction of the net hum level to well below one per cent of the maximum signal voltage.

We did notice that the manual hum compensation we employed was not stable over long periods of time--that is to say, that once zeroed, the hum level as detected by our amplifier gradually increased in magnitude. However, the amount of this buildup did not at all threaten to saturate the amplifier, and so the technique would appear to be perfectly good for a coarse compensation method. In conjunction with this coarse compensation method, however, one would then make use of phase-sensitive detection for ultimate, proper rejection of all hum voltage.

E. Noise in Flowing Dielectric

During the conduct of this experimental program we encountered a very considerable noise voltage which seems to be proportional to flow rate and exists even without energization of the magnetic field. This noise fortuitously turns out to be primarily of low frequency, and with even the most simple filtering it has been possible to filter it out so that it does not interfere with flowmeter operation at our induction frequency of 10 kc per second.

We have not been prompted to make a precise spectrum analysis of the above-cited electromagnetic noise, but nonetheless from visual observations of oscilloscope displays we conclude that the spectrum of the noise is approximately as indicated in Fig. 7 (note there that the ordinate is a linear scale and the abscissa is a logarithmic scale).

The spectrum indicated in Fig. 7 is decidedly similar to the turbulent velocity spectrum which one would expect with the pipe diameter and Reynolds number of the flow encountered in our flowmeter. Accordingly, we presume that this noise arises from frictional forces in the flowing dielectric. One explanation may be that foreign particulate matter--whether solid, liquid, or gas--possesses a density which is somewhat different from the density of the bulk liquid; consequently, an individual foreign particle would not follow a flow streamline precisely, and it may therefore be expected to acquire charge by frictional means. As the charge accumulation builds up on particles in a random fashion the electric fields associated with these charge accumulations can become quite large in the neighborhood of a particle. All is well until this localized electric field exceeds the dielectric strength of the bulk dielectric fluid--



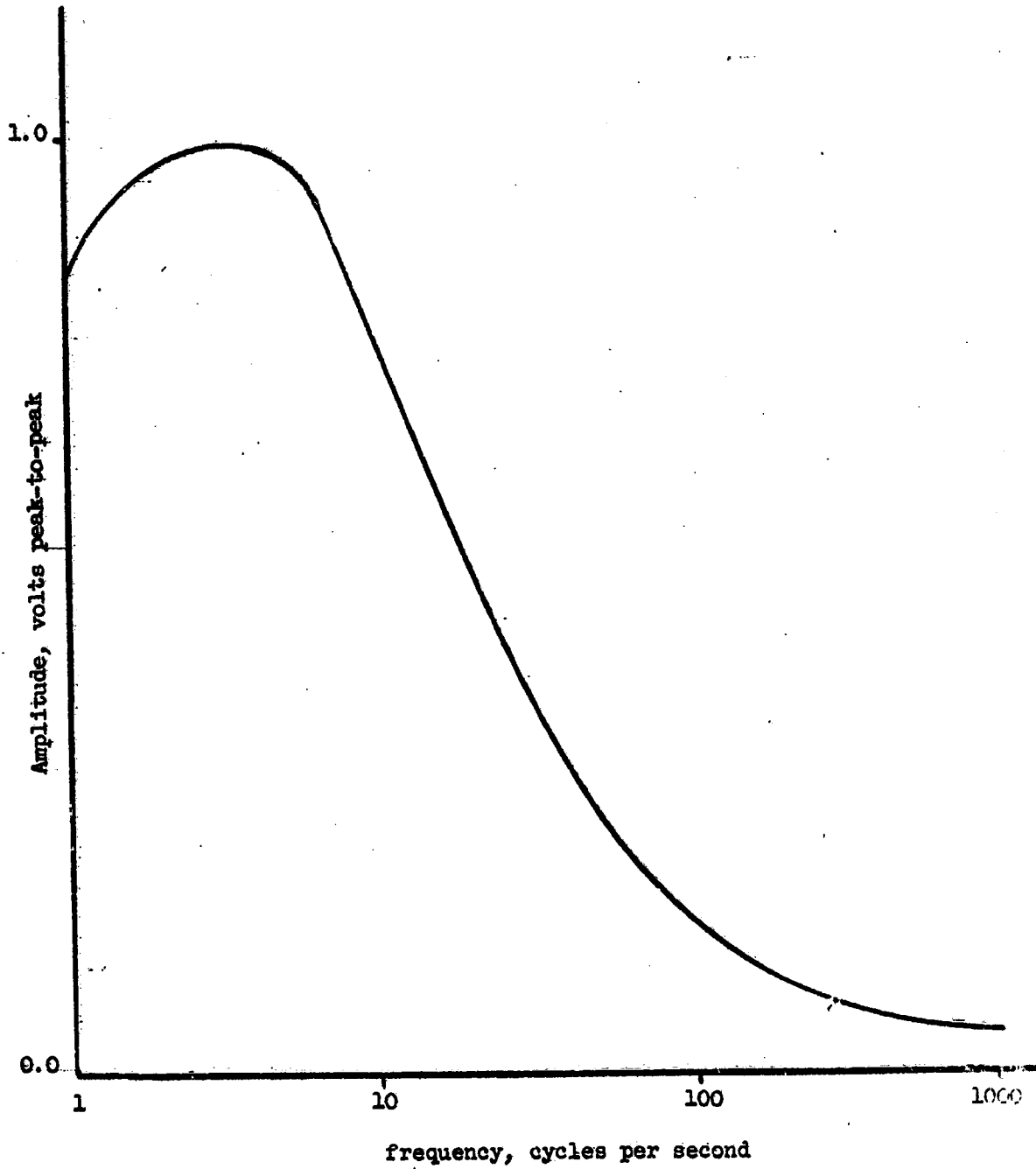


Fig. 7-- Approximate spectrum of electromagnetic noise.

thereafter lightning-like discharge takes place with associated electromagnetic radiation. We believe that it is this electromagnetic radiation due to random discharges, derived from turbulent flow of a dielectric, which is detected as flowing dielectric noise by the EM flowmeter's sensing electrodes.

Even though the intensity of this dielectric noise is small at the frequency of operation of the electromagnetic flowmeter, nonetheless it must be reckoned with in the design of any associated amplifier; again, if the amplifier should become saturated because of low frequency impressed voltages, the same amplifier would be quite useless as a linear device even at the operating frequency regime of 10 kc per second.

#### F. Expected and Measured Voltages

The flow induced voltage we have measured is, within experimental limits, in agreement with that to be expected from theoretical considerations. Equation (1) is in MKS units, and so proper care must be used in substituting English units of gpm and pipe diameter in inches. For typical experimental configurations we obtained a magnetic field strength of 80 gauss; in a flowmeter pipe of one inch diameter; at a flow rate of 50 gpm; and with electrodes which subtended a semi-angle,  $\beta$ , of  $70^\circ$ ; and from these values Eq. (1) would indicate an expected voltage of 990 microvolts. However, reference to the first term on the right of Eq. (6) would indicate that our measured voltage should be modified as indicated by the coefficient of  $e_p$ . For our particular electrode configuration we had [see Eqs. (4) and (5)]  $C_p \approx C_s \approx 0.5$  picofarads; while the value of  $C_a$ , the input capacitance to the amplifier, was approximately one picofarad.\* Therefore, the coefficient of  $e_p$  in Eq. (6) has the value one-fourth, so that overall we would expect our above-cited value of 990 microvolts to be reduced to approximately 240 microvolts.

The measured value under the above-cited conditions amounted to approximately half this value or 120 microvolts. Part of the discrepancy undoubtedly

---

\* Actually, the input capacitance to each half of our push-pull input amounted to approximately two picofarads; hence, the push-pull input capacitance amounts to one-half of this value or one picofarad.

can be explained by the inaccuracy in our knowledge of values for  $C_f$ ,  $C_s$ , and  $C_a$  in Eq. (6). But we believe that almost all of this difference can be ascribed to the fact that all of our analysis to date has been associated with a two-dimensional problem, i.e., one where all variables and parameters are invariant along the axial direction of the flowmeter. In respect to the magnetic field, this assumption certainly is not true in any practicable experimental configuration. As described in Section III B of this report (and as depicted in Fig. 12) the magnetic field is a maximum and quite nearly of constant amplitude throughout the middle two inches (in the axial direction) of the flowmeter pipe; but outside of this region the intensity of the magnetic field falls off rapidly. Thus, although our measured maximum magnetic induction amounted to some 80 gauss near the middle of the flowmeter pipe, its value fell off to considerably lower values than this near and beyond the extremes of the detecting electrodes--and in short the average or "effective" value of the magnetic induction is well below the maximum value of 80 gauss, and could easily account for the 2-1 discrepancy between our actually measured values of flow signal and our theoretically derived values based on a two-dimensional analysis.

In principle, of course, a three-dimensional analysis could be carried out; but in practice for useful configurations it would be most tedious, time-consuming, and expensive. Because of the linearity of the describing differential equations for the electromagnetic flowmeter we can be assured that, regardless of electrode configuration and magnetic configuration, any flowmeter voltage will be a linear function of volumetric flowrate through the pipe; and the constant of proportionality can be most easily ascertained by calibration tests. The one important condition for this linear performance, is that the transverse component of the magnetic induction be constant in (rms) amplitude throughout any given cross-section. But, importantly, this does not require that the transverse component of magnetic induction be the same at each cross-section of the flowmeter pipe; and indeed, as depicted in Fig. 12, in our experimental flowmeter the transverse component of magnetic induction does vary as we move up and down the pipe in the axial direction.

### III. FLOWMETER COMPONENTS

#### A. Housing and Fittings

The housing and end fittings (see Figs. 8 and 9) were constructed from aluminum because of its electrical characteristics and ease of machinability. Because of the two rigid triax leads emanating from the pipe/transducer, the housing was split axially for ease of assembly and disassembly. The housing was divided so that the plane lying between the half-sections was perpendicular to the magnetic flux path. This was done in accordance with high frequency electronic practice which requires that eddy currents established in the housing should not cross a cut in the conducting wall. The complete design and construction details are given in the First Quarterly Report<sup>4</sup> to the subject contract.

Four Amphenol Series C bayonet type coaxial connectors were installed at one end of the housing so that the two magnet coils could be connected either in series or parallel without disassembling the housing. To prevent the possibility of shorting between the magnet coils and the housing, a thin layer of mylar sheet was bonded to the interior surface of the housing.

The end fittings were designed to adapt to standard hydraulic tube fittings; specifically, 37° flared fittings 1-5/16 --12 UN-3A thread.<sup>5</sup> The static seal between the flowmeter pipe and the flow circuit was effected by an "O" ring groove and a flat teflon gasket.

The transducer preamplifier is mounted on four one-inch high metal spacers connected to one of the flat surfaces parallel to the plane lying between the two housing half-sections. In operation, the flowmeter housing, preamplifier chassis, and flow circuit (consisting of copper tubing) are electrically grounded through the earthing connection of the pump motor. The test flowmeter is coupled to the flow system by two flexible two-foot lengths of rubber hose clad with metal braid to provide electrical continuity over the entire flow circuit.<sup>6</sup>

---

<sup>4</sup>Vincent Cushing, Leo Di Gioia, and Dean Reilly, "Induction Flowmeter for Dielectric Fluids--Experimental Verification," First Quarterly Report issued by EPCO under Contract NASr-53, October 12, 1961, pp 2-3, Fig. 1.

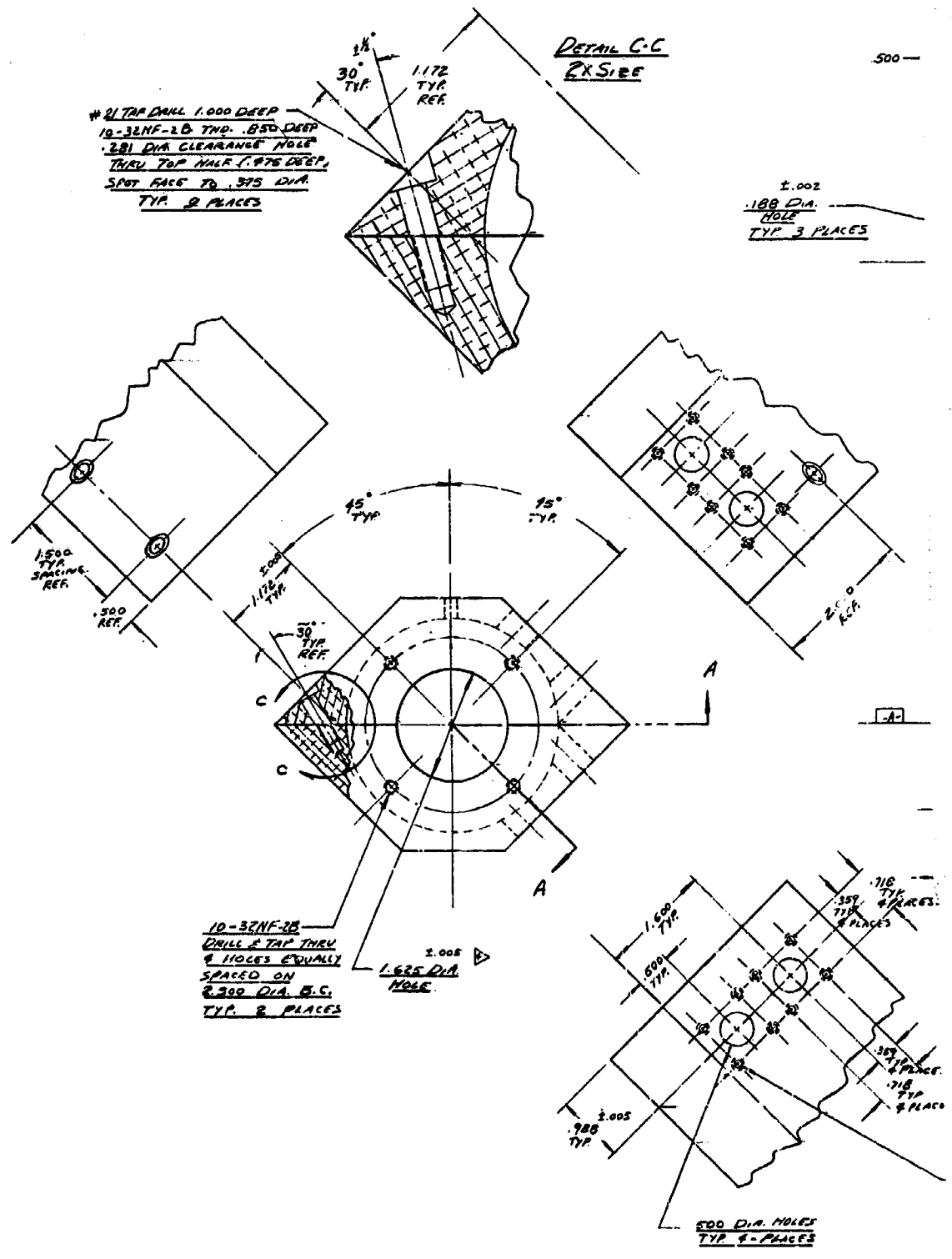
<sup>5</sup>Ibid, Fig. 2.

<sup>6</sup>Ibid, p 13.

DETAIL C-C  
RX SIDE

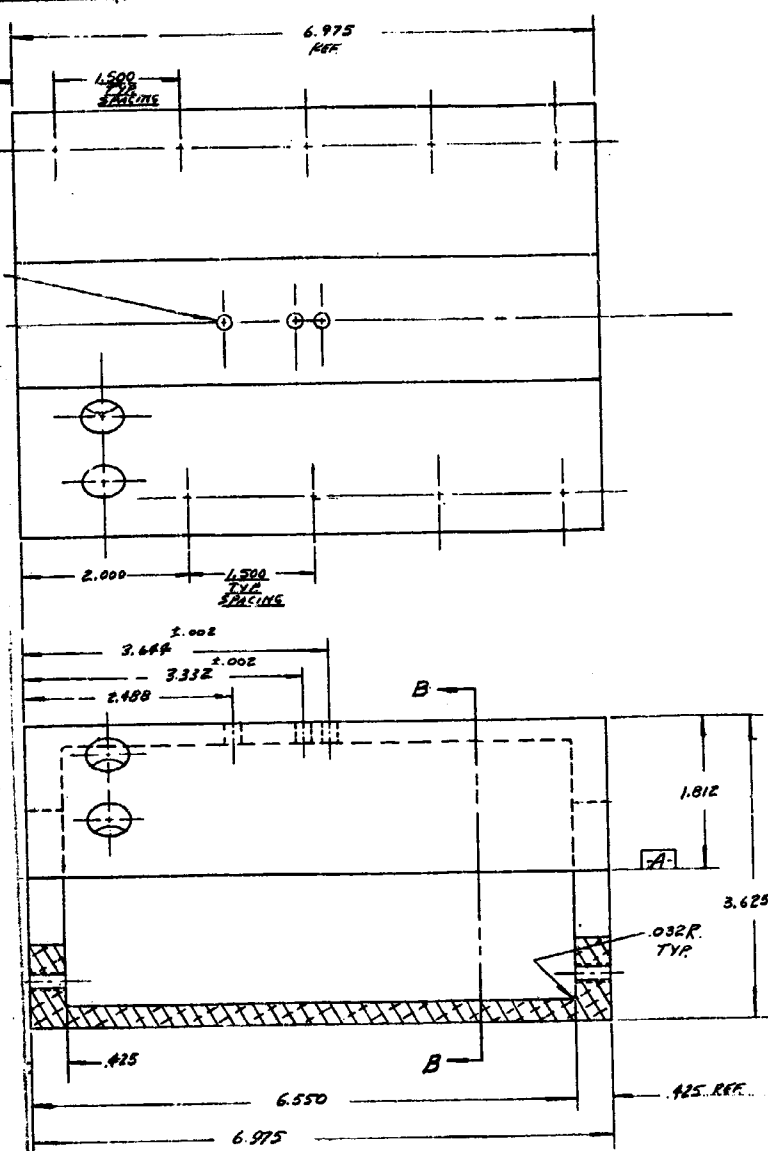
#21 TAP DRILL 1.000 DEEP  
10-32NF-28 THD. .850 DEEP  
.281 DIA CLEARANCE HOLE  
THRU TOP HALF (.975 DEEP,  
SPOT FACE TO .375 DIA  
TYP. 2 PLACES

±.002  
.188 DIA.  
HOLE  
TYP. 3 PLACES

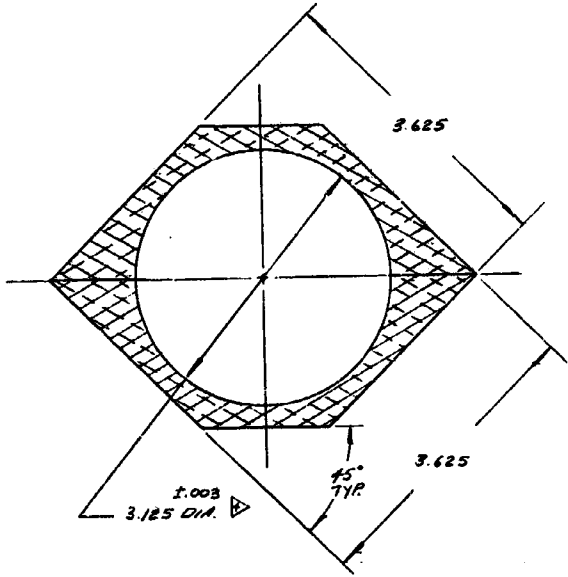


10-32NF-28  
DRILL & TAP THRU  
8 HOLES EQUALLY  
SPACED ON  
R.300 DIA. B.C.  
TYP. 2 PLACES

- 4. 1.625<sup>±.005</sup> AND 3.125<sup>±.002</sup> DIA. TO BE CONCENTRIC TO CENTERLINE  $\pm .010$  TYP.
  - 5. REMOVE ALL BURRS AND SHARP EDGES.
  - 6. TOLERANCES ON DIMENSIONS: DECIMALS ±.010, ANGULAR ±1° UNLESS OTHERWISE SPECIFIED.
  - 7. MATERIAL: ALUMINUM 2024-T3 OR EQUIVALENT.
- NOTES:



VIEW A-A

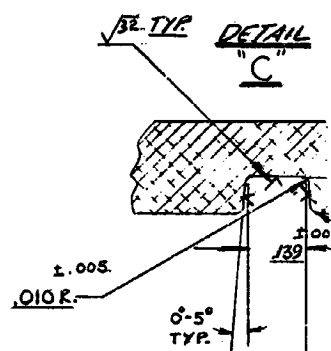
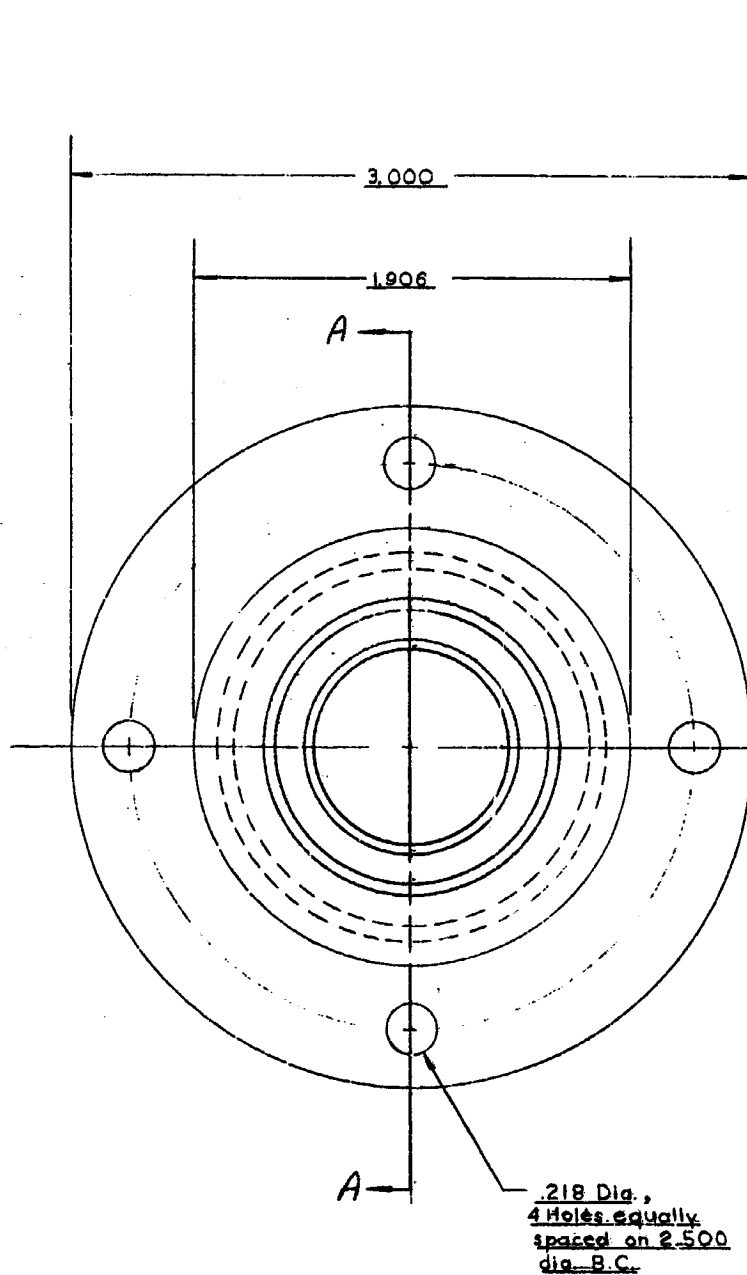


VIEW B-B

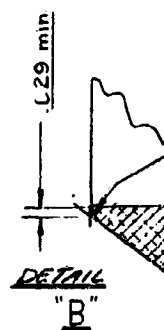
6-32NF-28  
 DRILL & TAP  
 .850 DEEP  
 6 HOLES  
 TYP. 4 PLACES

SCALE	1:1	METER HOUSING
TOL.	MITER	
MAPL	NOTE 1	EPCO-105-103
DRAWN BY	LO 9/4	ENGINEERING - PHYSICS Co ROCKVILLE, MARYLAND
CHECKED BY	10 9/4	

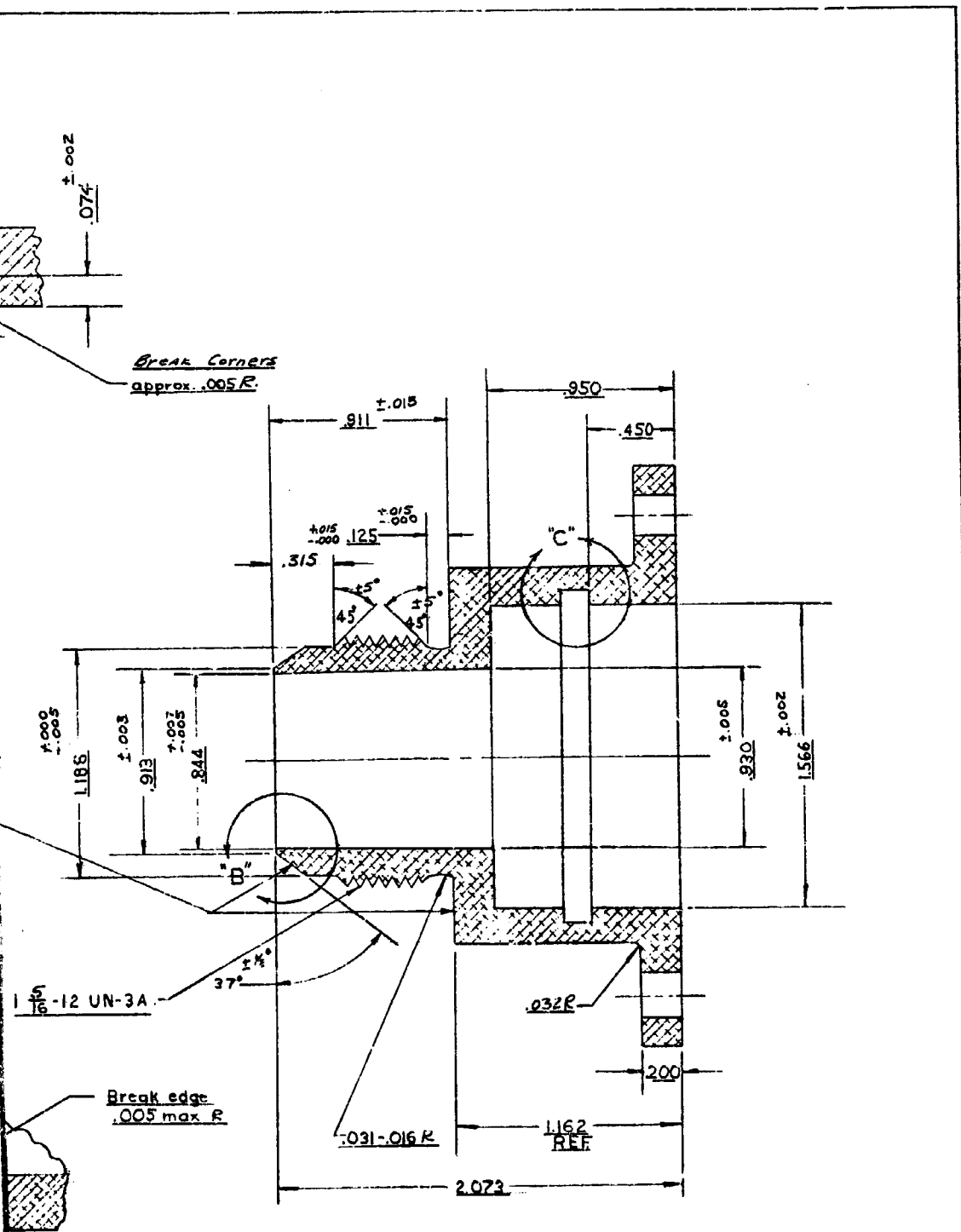
Fig. 8



This surface shall be free from burrs, longitudinal and spiral tool marks, and shall be smooth, except that angular tool marks will be allowed to 100 microinches RMS max.



1. TOLERANCE ON DIMENSIONS TO BE  $\pm .010$  UNLESS OTHERWISE SPECIFIED.
2. MATERIAL: ALUMINUM 2024-T4 OR EQUIVALENT.
3. REMOVE ALL BURRS AND SHARP EDGES.
- NOTES:



SECTION A-A

SCALE	2X	END FITTING
TOL.	±.010	
MAT'L.	Alum. 2024-T3	EPCO-105-102
DRAWN BY	RDP 7-64	ENGINEERING-PHYSICS CO.
CHECKED	GO 7-64	ROCKVILLE, MARYLAND

Fig. 9



## B. Magnetic Circuit

1. Magnet Coil Design--The magnetic field coils were wound on a coil form (furnished by the Engineering-Physics Company) by the Carol Electronics Company, Martinsburg, West Virginia, according to the design shown in Figs. 10 and 11. The design was dictated by the requirement that the maximum flux density required through the gap in the magnetic circuit be approximately 100 gauss at experimentally variable frequencies between 10 and 100 kcps. Low loss coils required the use of Litz wire. Calculations indicated that conditions would be satisfied if each coil half-section was composed of 57 turns of Litz wire constructed of 100 strands of AWG No. 34 copper wire. Each strand was covered with a 0.0005 inch thick coating of polythermaleze lacquer which has the combined advantages of high softening temperature and good dielectric properties. The overwrap consisted of a single layer of nylon filament. General Electric Type 1557 Glyptal Clear Lacquer was used as the bonding agent for the purpose of keeping the coils in the required shape, preventing the absorption of moisture, and improving the electrical insulation.

In order to produce a uniform magnetic field in the transducer, the coil cross-section was made to vary as a cosine function.<sup>7</sup> That is, the thickness of the coil diminishes as the cosine of the angle as shown in Fig. 10.

With a typical pair of 57 turn (half) coils connected in series and placed in the aluminum housing with a suitable magnetic return circuit (for details refer to the next section), the following electrical characteristics were measured:

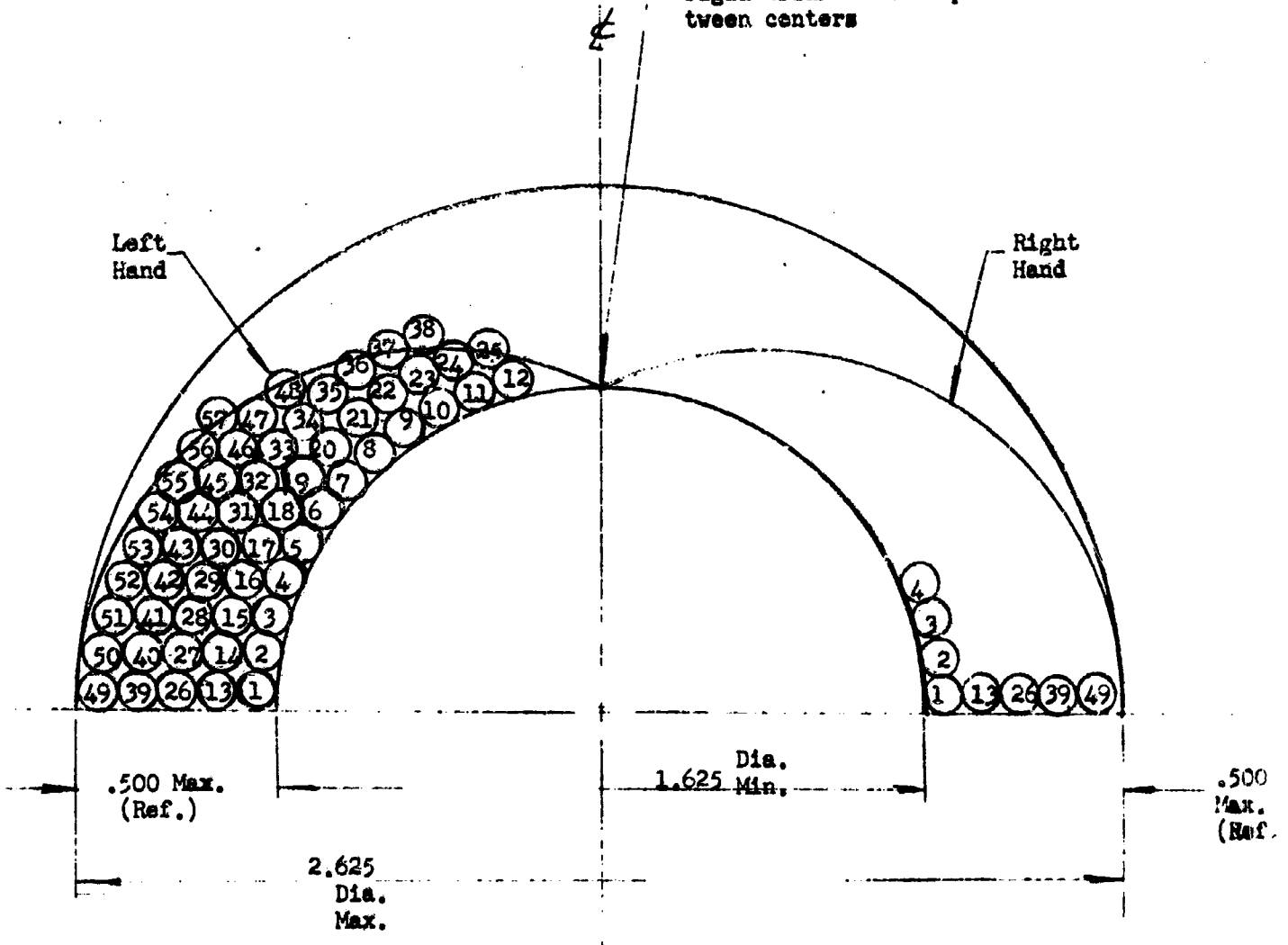
TABLE II

	<u>Electrical Properties of Magnet Coil</u>		
	<u>@ 1 kcps</u>	<u>@ 10 kcps</u>	<u>@ 100 kcps</u>
Inductance	0.95 mh	0.95 mh	0.93 mh
Q	10.2	41.0	136.0
D.C. Resistance (25°C)--0.361 ohms			

---

<sup>7</sup>Final Report for Contract NASr-13, March 22, 1961, p. 17.

Hole in center of coil half to allow clearance for two (2) .100 dia. rigid triax cables spaced .125 between centers



57 turns of Litz Wire  
(100 x A.W.G. No. 34)

Fig. 10--Magnetic coil cross section.

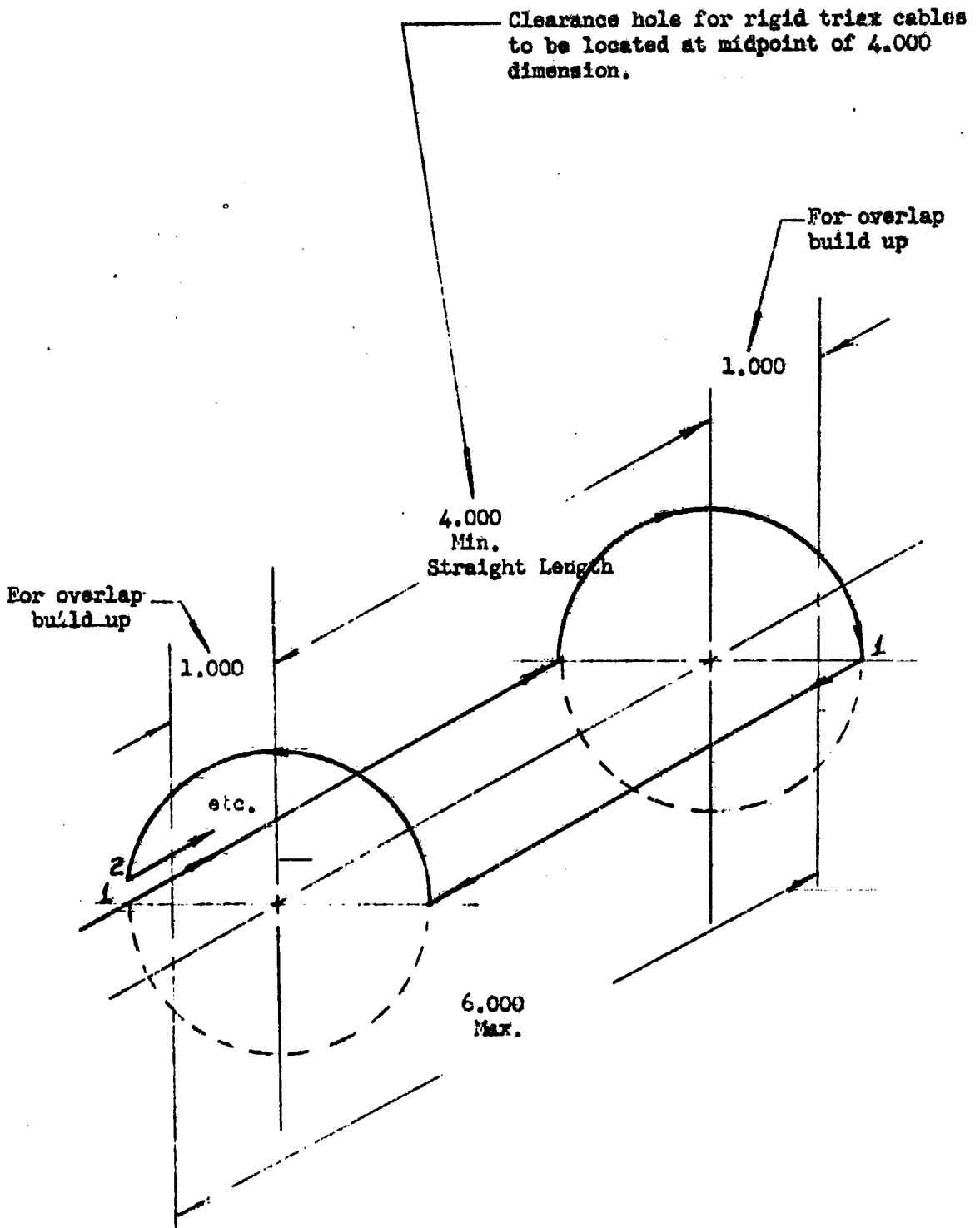


Fig. 11--Coil Winding Technique

It is seen from the table that the  $Q$  does not vary linearly with the frequency as it would if there were no skin-effect losses. This suggests the possibility of using a different Litz conductor comprising more strands of finer wire to further reduce these losses.

2. Magnet Circuit--To minimize the magnetomotive force required for operation of the magnet, a magnetic return path should be provided around the coil circumference. The original core material selected was a pressed and sintered molybdenum permalloy powder. Standard ring-cores were purchased from the Arnold Engineering Company and machined to the proper dimensions. Eight standard ring-cores were required for the magnet return circuit which were subsequently split into two equal halves (to permit assembly of the unit) and reduced in thickness to about 0.1 inch. In the experimental prototype work, the cost of having specially shaped cores could not be justified.

The permalloy material proved especially difficult to machine as well as being very brittle and hygroscopic. Hence, several different powdered iron core materials were purchased from Arnold. These were carbonyl L, C, and E alloys which are characterized by medium to high permeability, medium to high  $Q$ , and wide frequency range. Carbonyl L and C were found to machine well, and have since been used as the magnetic return circuit.

3. Magnet Power--Although any operational model flowmeter will employ a small, transistorized, fixed-frequency generator to provide an output of 5-20 watts, it was felt necessary to use a variable frequency power generator until the best operating frequency for the flowmeter could be experimentally determined. Therefore, an Acoustica, Model GU-400 ultrasonic generator was procured, which allows the output frequency to be continuously varied between 9 kcps and 1 mc.

As this generator was primarily designed to excite a large transducer of the type commonly employed in ultrasonic cleaning techniques, the manufacturers saw no need of suppressing the 60 cycle power supply ripple. It was necessary for us to suppress this modulation since, if it were allowed to circulate through the magnet coils, the flow signal itself would be modulated with this low frequency, in-phase voltage. Subsequent tests have indicated that this

modified generator is capable of stable excitation of the magnet coil in the frequency range previously specified.

To obtain sufficient current through the magnet circuit without overloading the generator, the Acoustica was connected across an L-C resonant circuit comprising the magnet coils and a parallel capacitance. The presence of relatively large circulating currents necessitated the use of low loss transmitting-type capacitors with mica, polystyrene, or teflon dielectric. As frequency stability is of premier importance, the temperature coefficient of the dielectric must be very low. In particular, metal encased polystyrene dielectric capacitors, manufactured by Film Capacitors, Inc., are exceptionally suited for this application due to their small size, high voltage rating, and low power factor.

4. Resultant Field--Figure 12 is a typical field plot indicating the strength of the transverse magnetic induction as a function of the axial position of field-sensing probe. The probe consists of a small 100 turn pickup coil covering an area of about one square centimeter and mounted at the end of a lucite rod which can be thrust into the interior of the pipe/transducer. The voltage applied to the magnet coils was measured on a Tektronix 531A oscilloscope as was the voltage induced in the pickup coil. From this graph it is seen that the magnetic induction has a constant (rms) value in a comparatively small region at the center of the magnet coils. Although the effective length of the coils is about four inches (the length of the core material) we should expect end effects to reduce the magnetic induction in the region approaching the ends of the coils.

Figure 12 shows the maximum value of the magnetic induction measured at the center of the coils as a function of the current through the coils. The current was measured with a Simpson radio-frequency ammeter connected in the resonant circuit. It is seen that the magnetic induction varies linearly with the coil current as is expected from Ohm's Law and Faraday's Law.

#### C. Pipe/Transducer

The theoretical aspects of the pipe/transducer have been discussed previously in the Final Report to EPCO's engineering analysis conducted under Contract NASr-13. Physically the pipe/transducer consists of three concentric

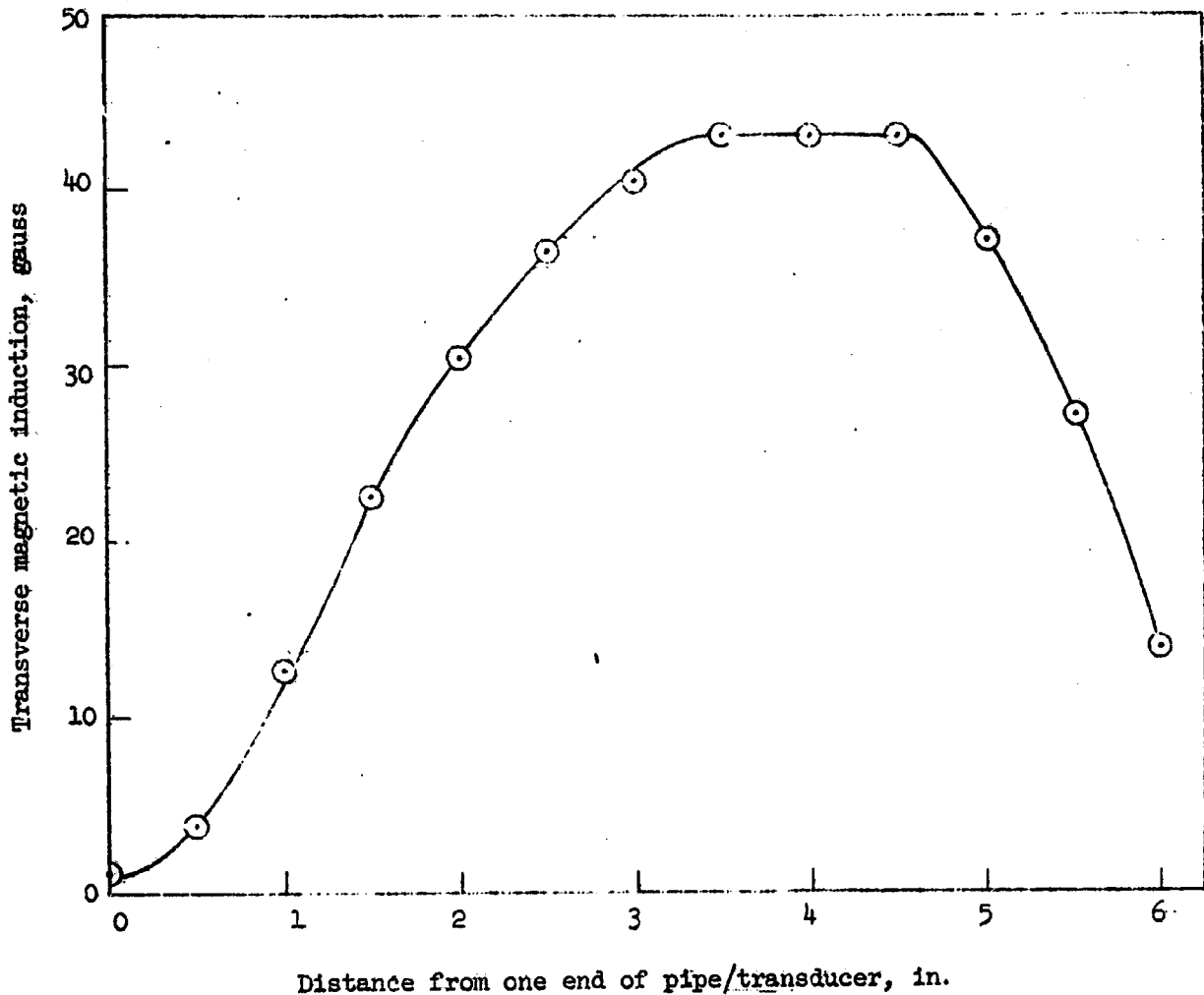


Fig. 12--Intensity of magnetic induction transverse to pipe/transducer. Transverse intensity is plotted as a function of axial position along pipe/transducer. Entire pipe/transducer is eight inches long; detection electrodes are positioned near central, uniform region. Measurements made with 114 turn coil at 10 kc; coil applied voltage of 150 volts.

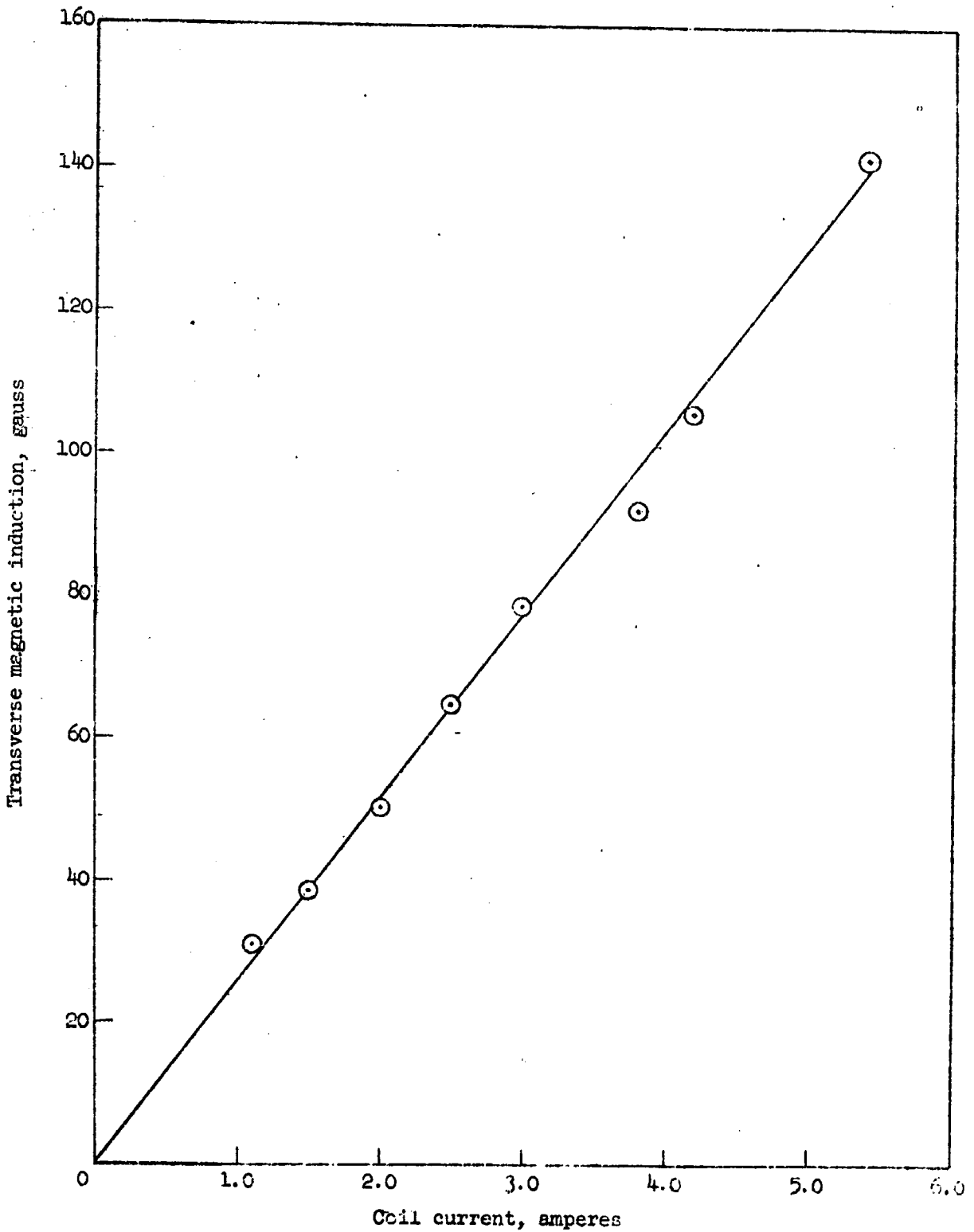


Fig. 13.--Maximum magnetic induction measured along transducer axis as a function of the current in the magnetic coil.

cylinders of dielectric material with electrodes bonded to their exterior surfaces. These electrodes are grid-like in form so as to allow the magnetic flux to pass undisturbed through the interior of the pipe. Two triaxial leads are connected to the electrodes and form an integral part of the transducer tube and provide a means of connecting the attendant detection circuitry.

More specifically the pipe/transducer as originally conceived, designed, and fabricated consists of a thin-walled cylindrical liner of teflon and two concentric fiberglass cylinders. Bonded to the teflon liner, inner-fiberglass cylinder, and outer-fiberglass cylinder respectively are a detecting electrode pair, a driven shield electrode pair and a ground grid.

Placing the electrodes on the surfaces of the fiberglass and teflon cylinders was the most difficult part of the transducer fabrication process. A five mil copper wire was wound on the fiberglass and teflon tubes in the form of a helix. After bonding these wires to the surface by means of an epoxy resin the unwanted portion was machined away allowing only the desired electrode area to remain. A single five mil wire was then used as a bus bar to connect the elements of the grid-like electrodes and this wire in turn was connected to the triaxial lead. Figure 14 shows the form of the electrodes manufactured by this technique.

The triaxial leads were formed from fine wire, copper foil, and teflon insulation. The edges of the copper foil are separated along a line parallel to the axial direction of the triaxial lead so as to prevent the induction of circulating currents due to the alternating magnetic induction. Figure 15 shows an end view of the triaxial leads. Two of these triaxial leads were used, each having the inner two conductors connected to a detecting electrode and driven shield electrode of one side of the pipe transducer. The outer conductor of both triaxial leads are fastened to the ground shield by connecting the two outer conductors together with a five mil wire, and in turn connecting one (and in this way avoiding a ground loop with circulating currents which might develop as a result of the alternating magnetic flux) of the conductors to the ground shield. The entire transducer is indicated in Fig. 16.

Using the symbols defined in Fig. 16, the characteristics of the transducer tube are given in Table III.



— Wire connecting electrode  
to triaxial lead

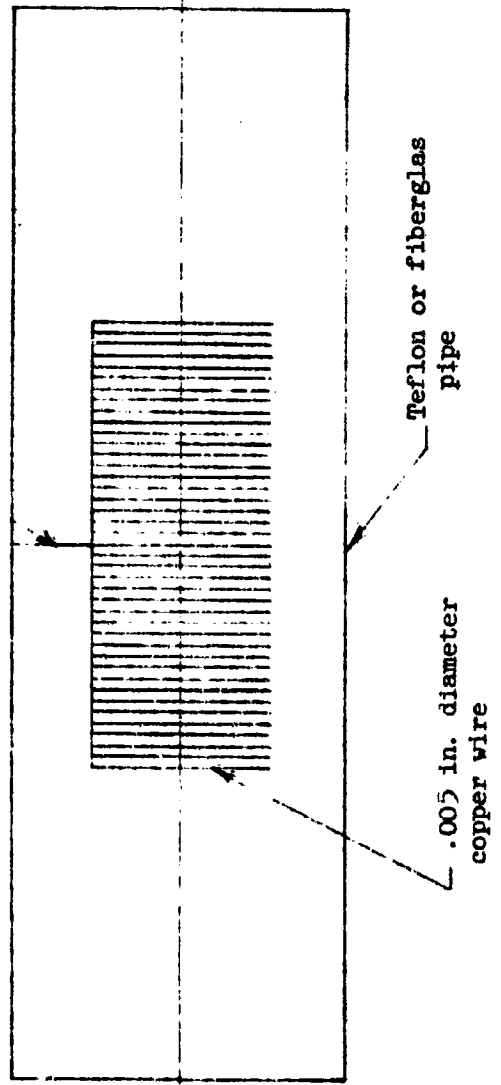


Fig. 14--Electrode configuration of detection and driven-shield grids.

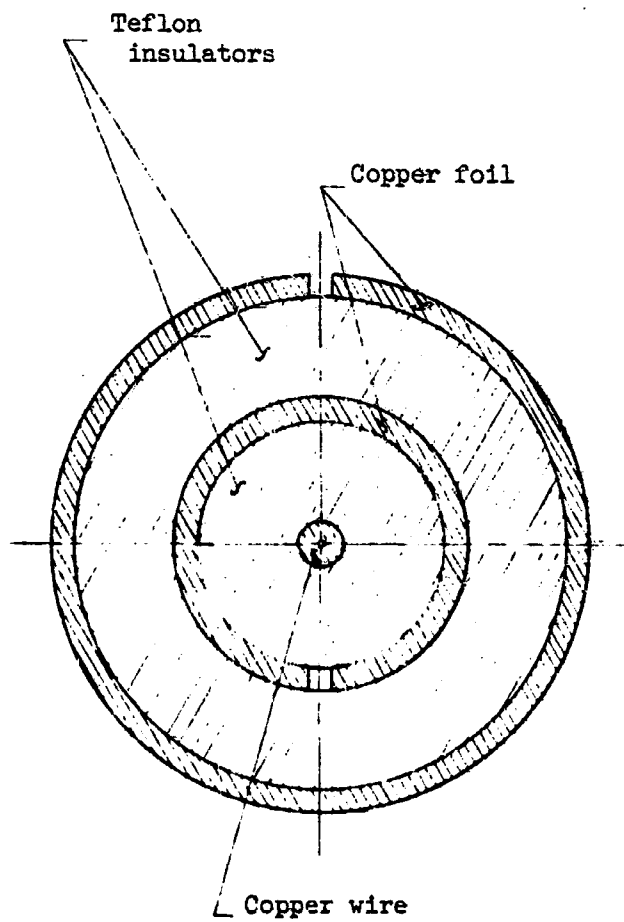
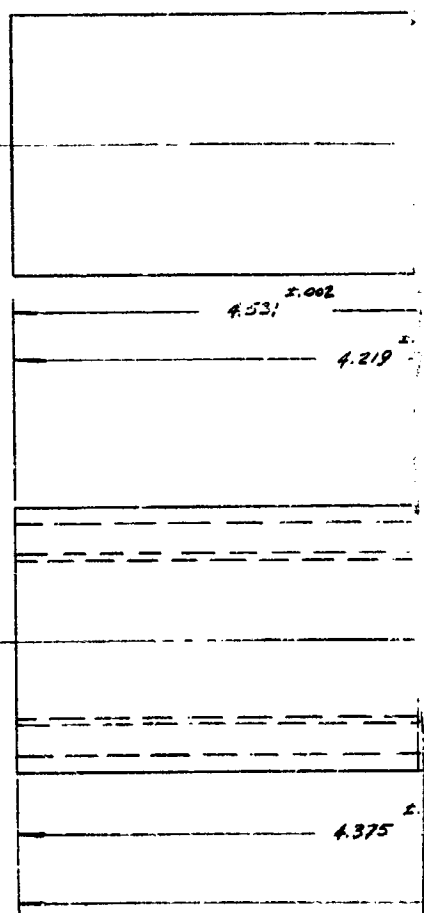
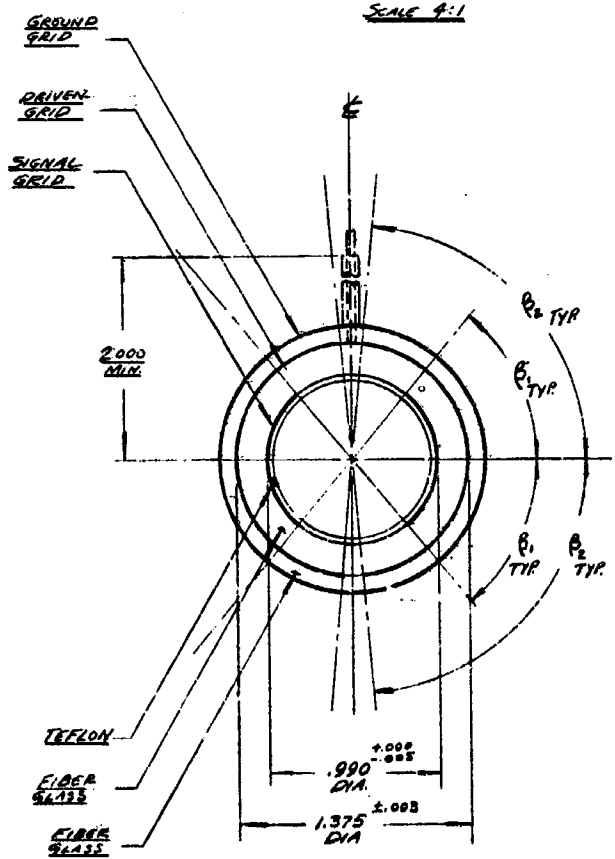
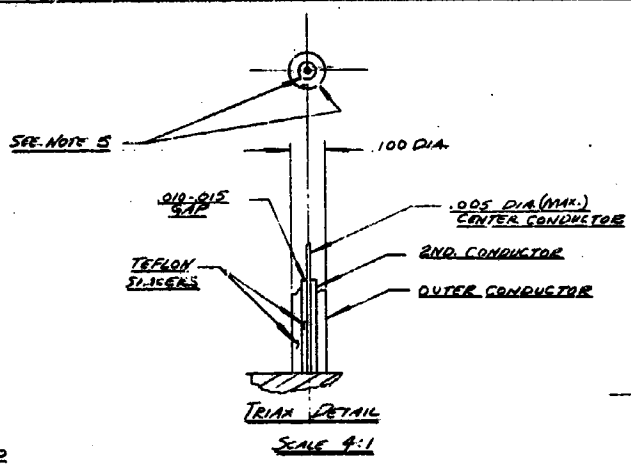


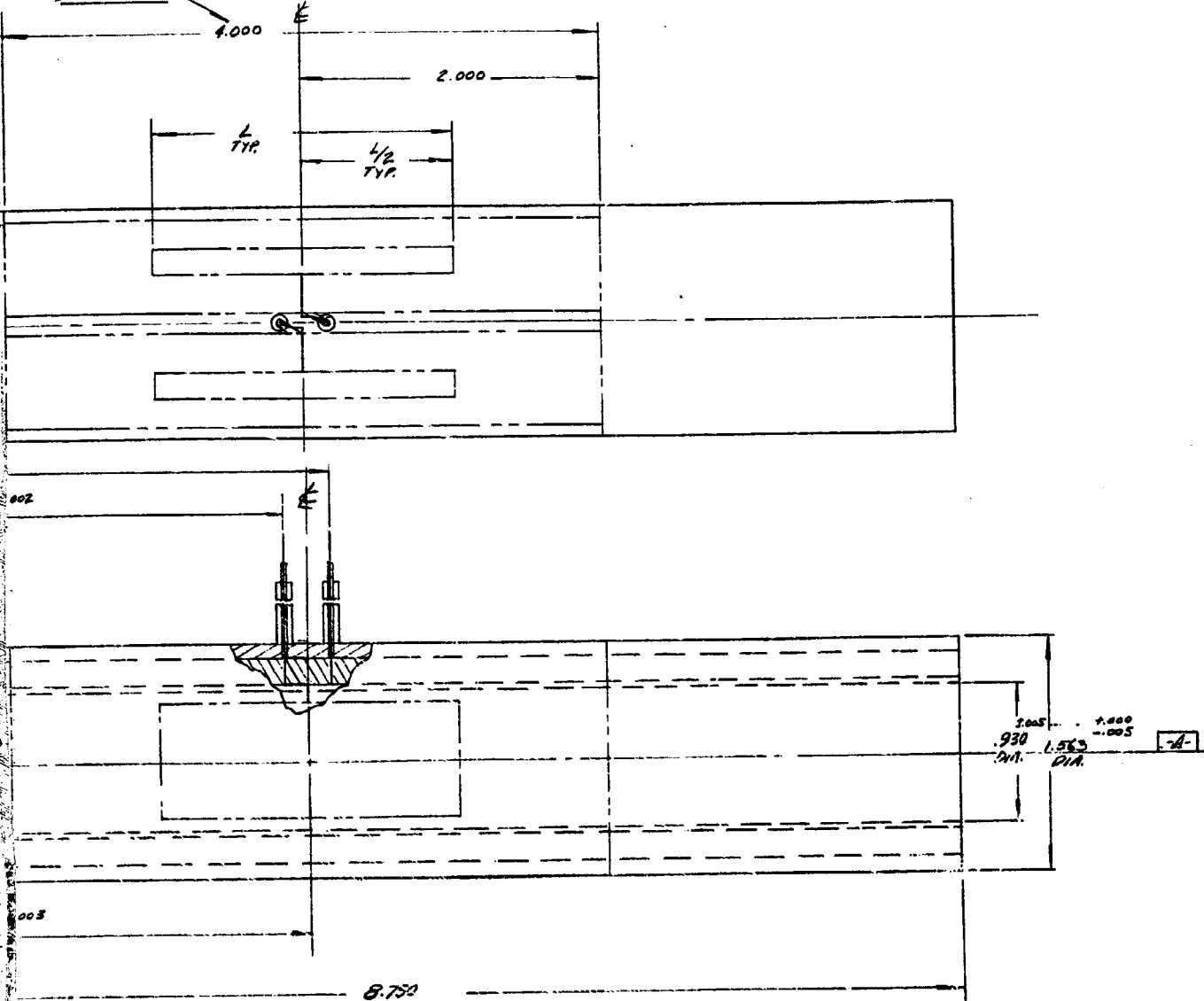
Fig. 15--End view of triaxial lead used to connect the pipe/transducer grids to the detection instrument.



2. ALL DIAMETERS TO BE CONCENTRIC TO -A- WITHIN 0.005 TYP.
6. COAT OUTER GROUND GRID WITH POLYETHYLENE FILM (TYP) FOR PROTECTION OVER 6.000 DIMENSION.
3. SECOND AND OUTER TRAX CONDUCTORS TO BE ELECTRICALLY DISCONTINUOUS ALONG A LONGITUDINAL LINE.
4. GROUND GRID TO ENCOMPASS 360 DEGREES.
3. ALL GRIDS TO BE CONSTRUCTED OF ELECTRICAL CONDUCTING MATERIAL CONTAINING A MINIMUM OF 100 LINES.
2. TOLERANCES ON DIMENSIONS: DECIMALS ±.010; ANGULAR ±1°, UNLESS OTHERWISE SPECIFIED.
1. MATERIAL: AS NOTED.

NOTES

SEE NOTE 6



$\beta_1$	50°	70°	85°
$\beta_2$	85°	85°	85°
L	2.900	3.000	2.500

PER INCH.

SCALE	2:1	METER PIN ASSY.
TOL.	NOTE	CPCO-105-10A
MARK.	NOTE	
DESIGNED BY	AD 1/11/41	ENGINEERING - PHYSICS CO.
CHECKED BY	AD 1/11/41	ROCKVILLE, MARYLAND

FIG. 16

TABLE III  
Mechanical and Electrical Characteristics  
of Pipe/Transducer

Electrode	Diameter, inches	Length, L inches	Angle,* degrees
detection	0.990	2.0	140
driven	1.375	5.0	150
ground	1.563	6.0	359

Electrode Pair **	Interelectrode Capacitance, *** picofarads	
	Side A	Side B
detection-driven	18	18
driven-ground	82	82

D. Amplifier

The amplifier circuit, as indicated in Fig. 17 consists first of all of a two-stage capacitance-coupled amplifier employing vacuum tubes V1 and V2. The entirety of the forward gain is fed back degeneratively into the cathode of the first stage. As the electromagnetic flowmeter provides a push-pull signal, we have accordingly employed a push-pull input to the amplifier; i.e., we have, symmetric with the previously described amplifier, an identical two-stage, feed-back stabilized amplifier incorporating the pentodes, V3 and V4.

Because of the very large amount of feedback employed in the first two stages, the gain of these is virtually unity--actually being something like 0.99.

\* Full angle subtended by curvilinear electrode.

\*\* On page 9 we computed the capacitance between detection electrode on side A and detection electrode on side B; this quantity, because of various stray capacitances, is difficult to measure directly. However, the interelectrode capacitances cited in Table III do agree with corresponding theoretical estimates.

\*\*\* Measured with General Radio Bridge Model 1650A.

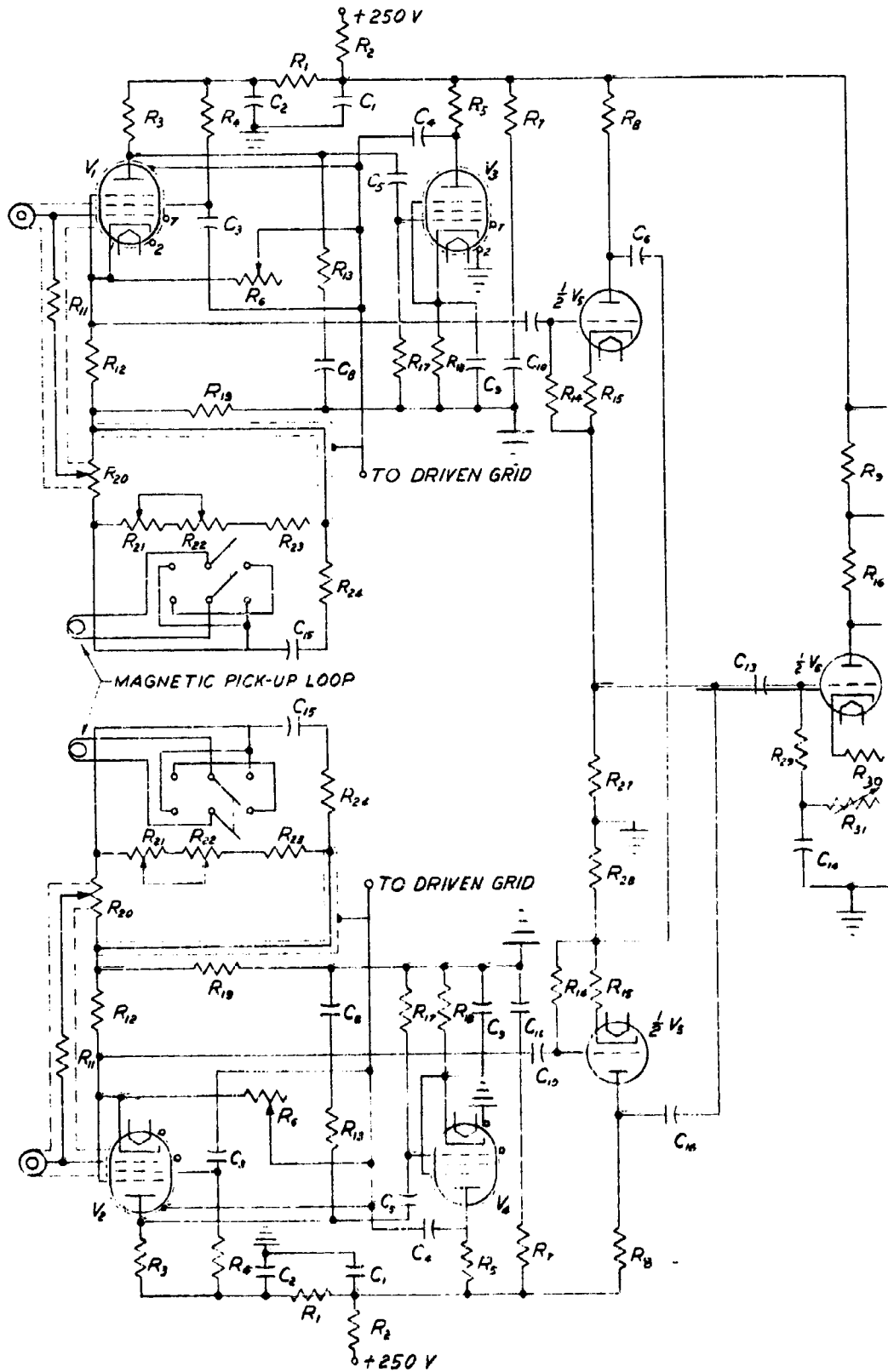
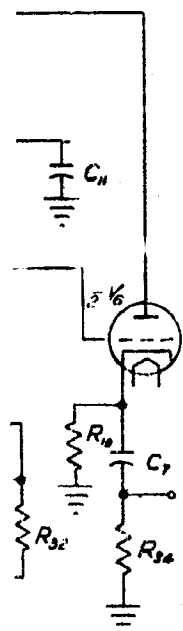


Fig. 17--Schematic of amplifier used for detection of flow signal.



R <sub>1</sub>	27K	R <sub>28</sub>	68K	C <sub>1</sub>	150μf
R <sub>2</sub>	2.2K	R <sub>29</sub>	1M	C <sub>2</sub>	2μf
R <sub>3</sub>	22K	R <sub>30</sub>	1.3K	C <sub>3</sub>	2μf
R <sub>4</sub>	220K	R <sub>31</sub>	0-100K	C <sub>4</sub>	20μf
R <sub>5</sub>	22K	R <sub>32</sub>	47K	C <sub>5</sub>	3000μμf
R <sub>6</sub>	0-5K	R <sub>33</sub>	1.3K	C <sub>6</sub>	4μf
R <sub>7</sub>	68K	R <sub>34</sub>	100K	C <sub>7</sub>	1μf
R <sub>8</sub>	68K			C <sub>8</sub>	270μμf
R <sub>9</sub>	15K			C <sub>9</sub>	.01μf
R <sub>10</sub>	160K			C <sub>10</sub>	1μf
R <sub>11</sub>	22M			C <sub>11</sub>	4μf
R <sub>12</sub>	2.2K			C <sub>12</sub>	4μf
R <sub>13</sub>	2.2K			C <sub>13</sub>	.05μf
R <sub>14</sub>	1.0M			C <sub>14</sub>	1μf
R <sub>15</sub>	1.3K			C <sub>15</sub>	.01μf
R <sub>16</sub>	68K			C <sub>16</sub>	4μf
R <sub>17</sub>	22M				
R <sub>18</sub>	330Ω				
R <sub>19</sub>	47K				
R <sub>20</sub>	0-50K				
R <sub>21</sub>	0-20K				
R <sub>22</sub>	0-2K				
R <sub>23</sub>	1.5K				
R <sub>24</sub>	1.5K				
R <sub>25</sub>	68K				
R <sub>26</sub>	1M				
R <sub>27</sub>	68K				

V<sub>1</sub> thru V<sub>4</sub> = 6X4  
 V<sub>5</sub>, V<sub>6</sub> = 6112

This very large amount of negative feedback in the first two stages provides the desired high input impedance in addition to providing an effective input capacitance of the order of 5 picofarads. The push-pull output of the first two push-pull stages is obtained from the cathodes of tubes V1 and V3.

It is common practice when employing a driven shield--such as we utilize in the electromagnetic flowmeter design and attendant transmission line to the input of the amplifier--to connect the driven shield to the output of a highly stabilized, unit-gain amplifier (i.e., in this case connected to the cathode of our two stage amplifier). The purpose of this driven shield is to cause a considerable reduction in the effective value of the capacitance between the transmission line and its surrounding shield. In addition--as was indicated in an earlier report<sup>8</sup>--we can also reduce the effective input capacitance of our amplifier to the ideal value of zero by driving the shield from an amplifier whose gain is very slightly greater than unity. The net effect is that the slightly overdriven shield effectively gives rise to a negative capacitance, and this capacitance is so adjusted that it cancels the small natural, positive capacitance normally encountered. As shown in Fig. 17, the driven shields are electrically connected to the high side of the rheostat, R<sub>6</sub>. The proper amount of overdrive on the shield may be adjusted by adjusting the rheostat.

With the rheostat shorted out so that the driven shield is connected to the cathode of the first stage, we have, as has already been described, an input capacitance of about 5 picofarads. However, by adjusting the aforementioned rheostat, it is possible to reduce the effective input capacitance--as measured on a General Radio bridge--of our amplifier to approximately 1 or 2 picofarads, depending upon the frequency employed. It should be possible to reduce the effective input capacitance even further, perhaps by a factor of 20 or more, if careful attention is given to the slight phase shift which appears to take place in our preamplifier with the net effect that the driven shield is not driven precisely in phase with the signal voltage. In a fixed frequency amplifier, which

---

<sup>8</sup> Vincent Cushing, Leo Di Gioia, and Dean Reilly, "Induction Flowmeter for Dielectric Fluids--Experimental Verification," First Quarterly Report, loc. cit.



would be used in any practical application, it would appear that the effective input capacitance for the attendant amplifier can be reduced to a much lower value by proper adjustment of the phase shift at the fixed operating frequency.

Also, it should be mentioned that 1 picofarad is the limit of resolution for the General Radio 1650A bridge which we have used to make our capacitance measurements; hence, our measured limitation of 2 picofarads may be partially due to measurement limitation.

As seen in Fig. 17, the push-pull output of the feedback-stabilized first two stages is fed into the common mode rejector circuit built around the twin triode, V5. This common mode rejector at the same time provides a single-sided output which is proportional to the differential input voltage to this stage. The output of the common mode reflector is then fed into a conventional triode amplifier built around one-half of the twin triode, V6. The output of the triode stage is in turn fed into the cathode follower circuit as shown. The cathode follower has the virtue of a quite low output impedance for transmission of the amplified flow signal over a considerable length of transmission line if desired.

It should be noted that the amplifier currently in use was purposely designed for test purposes with a capability for experimental operation over a wide band of frequencies. Hence the operating frequency of the flowmeter can be varied between 10 and 100 kcps so that the best operating frequency for the final operational model could be determined. Such a wideband amplifier, as is well known, accepts and amplifies a considerable amount of noise, including the electrical static noise generated in any flowing dielectric.

For an operational flowmeter, we plan to develop a tuned, fixed-frequency, gain stabilized low noise amplifier. For ruggedness, reliability, and compactness, transistors will be employed throughout except for the first stage, where requirements for a high input impedance and low input capacitance requires one to employ vacuum tubes.

#### E. Hum Compensator

As discussed in the final report to Contract NAS-13,<sup>9</sup> there is practically always a concomitant hum voltage due to the so-called transformer effect.

---

<sup>9</sup>Vincent Cushing and Sean Reilly, "Induction Flowmeter for Dielectric Fluids--Engineering Analysis," loc. cit.

This hum voltage is in quadrature with the flow induced signal voltage, and therefore, in any fixed frequency flowmeter, may be rejected by the use of a phase-sensitive detector. However, if the hum voltage is large it is possible that the amplifier will become saturated before the phase-sensitive detector may be utilized; therefore, it is desirable to provide an approximate, manually adjusted hum-bucking voltage at the grid of the first stage of the amplifier. By reference to Fig. 17, the proper magnitude of this bucking voltage is injected into the grid by means of the potentiometer,  $R_{20}$ . The voltage which is injected at this point is originally derived from a single loop (placed on the outside surface of the pipe/transducer) which provides a voltage induced by the alternating magnetic induction. Generally, in practice, there is a small amount of phase difference between the hum voltage picked up by this sensing loop and the hum voltage detected in the flowmeter circuit. Accordingly, a phase shift network consisting of the fixed resistors,  $R_{23}$  and  $R_{24}$ , the rheostats  $R_{21}$  and  $R_{22}$ , and the fixed capacitor  $C_{15}$  is employed. The output of this network is then fed into the potentiometer,  $R_{20}$ , for injection into the grid of the first stage.

#### F. Associated Electronic Equipment

Figure 18 is a block diagram of the equipment used in the flow detection circuit. The cathode-follower output of the preamplifier is fed through a narrow band-pass filter to a Keithley 102B decade isolation amplifier with a maximum gain of 1000. The output of the Keithley is fed through a second filter to the oscilloscope input. In the early stages of flow detection it has been helpful to analyze the flow signal waveshape on an oscilloscope as well as its amplitude; whereas, in later models a d-c meter movement will be used as the output detector.

The band-pass filters used in the flow detection tests at 10.5 kcps were United Transformer Company type TMN 10.5, having a pass-band of 800 cycles and an attenuation of 40 db per octave on either side of the center frequency. The filter between the preamplifier and isolation amplifier acted to reduce the wide band noise inherent in the preamplifier and the electrification noise generated in the fluid itself. The filter at the output of the Keithley amplifier attenuated the off-frequency amplifier noise of 50 microvolts. The noise remaining in the pass band--with an overall amplifier gain of 20,000--was 25 microvolts

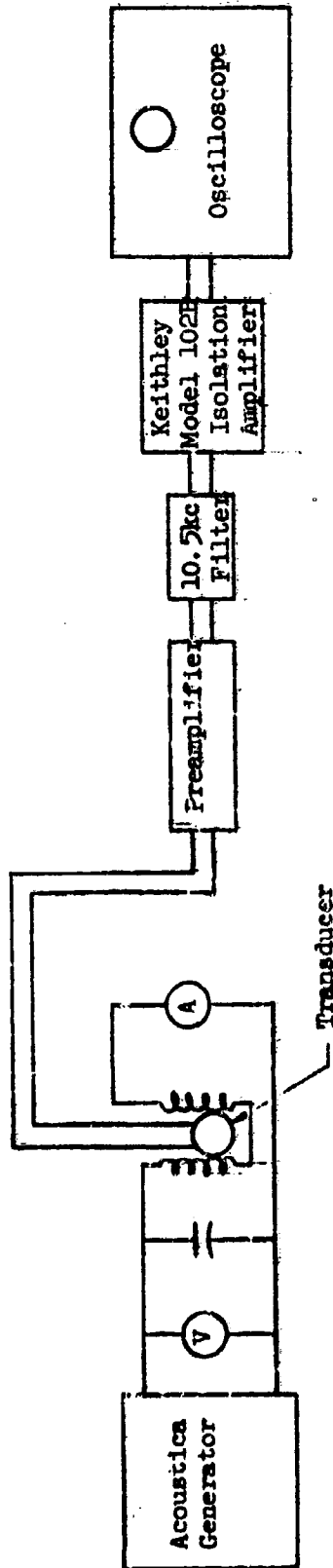


FIG. 18--Prototype flowmeter test circuit.

as referenced to the input of an ideal amplifier with a 20,000 gain factor. In future fixed frequency amplifier designs it will be possible to reduce this noise figure by at least an order of magnitude to achieve a better signal-to-noise ratio. This is possible with now available low-noise transistor amplifier stages, and frequency selectivity introduced suitably into the preamplifier.

#### IV. CONCLUSIONS AND RECOMMENDATIONS

The concept of an electromagnetic flowmeter for use with dielectric fluids-- and in particular the cryogenic propellants--as proposed to NASA by the Engineering-Physics Company, has been experimentally verified and found to be practicable. The most critical problem, as one would perhaps expect from the outset, was in the development of fabrication techniques for the pipe/transducer. Once this problem was solved, the remainder of the experimental endeavor moved along essentially in accord with the theory developed earlier under Contract NASr-13.

Except for the pipe/transducer, the remainder of the components in the electromagnetic flowmeter consist of readily available items and electronic systems. However, somewhat of a limitation from an electronic point of view has been the realization that quantitatively accurate voltage measurements in the millivolt regime are limited, at today's state of the art, to frequencies at and below approximately 10 kc per second. The state of the art generally in respect to frequency is moving toward higher frequencies, and our ultimate requirement of, say, 50 or 100 kc per second should be attainable within the next year or two. But meantime, our current operation at 10 kc per second allows quite adequate operation of the electromagnetic flowmeter in all respects, with the one proviso that measurement of flow oscillation is currently limited to something like 100-200 cps.

In the Engineering Analysis carried out under Contract NASr-13, we talked in terms of magnetic field strengths in the neighborhood of 100-150 gauss; and with consequent flow induced voltages in the neighborhood of 3-4 millivolts. We have come to find out that, with a bandwidth in the attendant detector-amplifier limited to 100-200 cps, the extraneous electrical noise in a generally achievable narrow band amplifier is of the order of one microvolt or less; and we should thus be able to operate with full flow signals of the order of 200-300 microvolts. The

implication is that we can get along with 5-10 gauss of magnetic field, and this in turn promises a magnet coil and attendant power generator of quite small proportions.

In addition to the unique capabilities of the basically volumetric electromagnetic flowmeter, we have noted that, since hydrogen, oxygen, fluorine, nitrogen, and most of the constituents of RPl consist of non-polar molecules, it is possible to embellish the electromagnetic flowmeter, by means of monitoring the bulk dielectric constant, so that it becomes a mass-rate meter. Yet another embellishment would be the development of an electrical two-phase flowmeter system; as described in Section II of this report this would have the net effect of averaging out inhomogeneities in the flowing fluid, so that one could measure flow rate in the face of hydrodynamically two-phase flow of arbitrary velocity profile.

Although the electromagnetic flowmeter can be embellished to possess capabilities which are inherently difficult or unobtainable with other principles of flowmeter operation, nonetheless we believe that the next step in development should be the design, construction, and test of an EM flowmeter configuration which would be practicable for use with liquid hydrogen in rocket test stands. The flowmeter configuration we have used in this experimental verification phase is made up of components which were designed primarily for experimental flexibility rather than operational ruggedness, compactness, reliability, and economy. We believe now that a fixed-frequency flowmeter for operational use should be developed with the four last-cited virtues in mind.